CAPÍTOL 2

Identification and characterization of human eosinophil cationic protein by an epitope-specific antibody

Ester Boix, Esther Carreras, Zoran Nikolovski, Claudi M. Cuchillo, and M. Victòria Nogués

Departament de Bioquímica i Biologia Molecular, Facultat de Ciències, Universitat Autònoma de Barcelona, 08193-Bellaterra, Spain

Abstract: The eosinophil cationic protein (ECP) is a basic secretion protein involved in the immune response system. ECP levels in biological fluids are an indicator of eosinophil-specific activation and degranulation and are currently used for the clinical monitoring and diagnosis of inflammatory disorders. A polyclonal epitope-specific antibody has been obtained by immunizing rabbits with a conjugated synthetic peptide. A sequence corresponding to a large exposed loop in the human ECP three-dimensional structure (D115–Y122) was selected as a putative antigenic epitope. The antibody was purified on an affinity column using recombinant ECP (rECP) as antigen. The antibody (D112–P123 Ab) specifically recognizes rECP and its native glycosylated and nonglycosylated forms in plasma, granulocytes, and sputum. The antibody detects as little as 1 ng of rECP, can be used both in reducing and nonreducing conditions, and does not cross-react with the highly homologous eosinophil-derived neurotoxin or other proteins of the pancreatic ribonuclease superfamily. *J. Leukoc. Biol.* 69: 1027–1035; 2001.

Key Words: *immunoassay · granulocytes · plasma · sputum*

INTRODUCTION

Eosinophils are major effector cells in the inflammatory response. The eosinophil cationic protein (ECP) is a basic protein located in the eosinophil primary matrix and is involved in the immune response system. Eosinophil secretion proteins are active in the host defense mechanism against bacterial, helminthic, and viral infections. The cytotoxicity of ECP can also damage the epithelial host cells, and eosinophils are considered the primary leukocytes responsible for tissue damage in inflammatory diseases (reviewed in ref. 1 and 2). Eosinophil recruitment and degranulation have been correlated with the pathogenesis of asthma and inflammation due to viral infections [3, 4]. The specific release of granule secretion proteins by activated eosinophils has been analyzed by measuring ECP levels in biological fluids and noting its correlation with several eosinophil cell effectors, such as immunoglobulins and components of the complement system [5, 6].

The ECP sequence shows a high homology with the sequence of the eosinophil-derived neurotoxin (EDN), another protein of the eosinophil granule matrix. Both ECP [also known as ribonuclease (RNase) 3] and EDN (also known as RNase 2) are ribonucleolytic enzymes belonging to the pancreatic RNase (EC 3.1.27.5) superfamily. ECP has three potential glycosylation sites for asparagine-linked oligosaccharides, and three glycosylated forms of native ECP (with 18-, 20-, and 22-kDa molecular masses) have been described [7, 8]. Recent studies suggest that the differential glycosylation of ECP may be critical for the regulation of its biological function [2].

ECP levels in serum, sputum, and other fluids are currently used as markers for the diagnosis and monitoring of the therapeutic efficacy in acute- and chronic-inflammation diseases, as well as other hypereosinophilia syndromes [2]. Several antibodies designed to determine the ECP levels in biological samples have been described. Monoclonal antibodies EG1 and EG2 have been used in clinical studies for the detection and quantification of ECP [9]. These antibodies were raised against either eosinophil extracts or the eosinophil granule products, and their recognition capabilities are discussed below. An enzyme-linked immunosorbent assay (ELISA) using polyclonal antibodies against purified native ECP has also been described [10]. Pharmacia & Upjohn (Uppsala, Sweden) developed an improved immunoassay for ECP detection (Pharmacia CAP System™) [11], and a fully automated assay that combines immunoglobulin (Ig) E with other allergy markers is currently being used for the monitoring of allergy immunotherapy (UniCAP™, Pharmacia & Upjohn) [12]. However, the lack of information on the epitope involved in the immune detection system and the lack of specificity of the assays reduce some of the potential applications of these methods for basic research studies.

We have developed a specific antibody against a defined region of ECP. This antibody does not cross-react with either EDN or the other proteins of the pancreatic RNase superfamily, but it detects both the glycosylated and nonglycosylated forms of ECP, either native or denatured. The selected epitope

Correspondence: M. Victòria Nogués, Departament de Bioquímica i Biologia Molecular, Facultat de Ciències, Universitat Autònoma de Barcelona, 08193-Bellaterra, Spain. E-mail: victoria.nogues@uab.es

Received March 24, 2000; revised January 29, 2001; accepted January 31, 2001.

was chosen according to a prediction model of the ECP three-dimensional structure [13] based on the EDN three-dimensional structure [14]. The sequence D115–Y122 corresponds to a unique exposed region, which is a specific large insertion loop in eosinophil-associated RNases and in RNase K6 [15] (**Fig. 1A** and **B**). The epitope was further characterized by an analysis of the X-ray crystal structure of ECP (Fig. 1A) [16]. Rabbit polyclonal antibodies were obtained with an ECP synthetic peptide, and antibodies were further purified by affinity chromatography using immobilized recombinant ECP (rECP). We have characterized the antibody by ELISA, dot blotting, sodium dodecyl sulfate (SDS)-polyacrylamide gel electrophoresis (SDS-PAGE), and Western blotting. Plasma, granulocytes, and sputum samples have been analyzed with this antibody.

MATERIALS AND METHODS

EDN that had been extracted from human eosinophil granules was the generous gift of Gerald Gleich. RNase A (type XII), poly(C), poly(U), baker's yeast RNA (type XI), protein molecular weight markers, 3-dimethylaminobenzoic acid, and 3-methyl-2-benzothiazoline hidrazone were purchased from Sigma Chemical Co. (St. Louis, MO). Diethylaminoethyl-Sepharose CL-6B and protein A-Sepharose CL-6B resins, PD10, HiTrap Q, and HiTrap SP prepacked columns, and Hyperfilm-MP (high-performance autoradiography film) were from Amersham Pharmacia Biotech (Uppsala, Sweden). Limphoprep was obtained from Nycomed Pharma AS Diagnostics (Oslo, Norway). Monoclonal antibody EG1 was from Kabi Pharmacia Diagnostics AB (Uppsala, Sweden). Amplified alkaline phosphatase goat anti-rabbit immunoblot assay kits and goat anti-mouse antibody conjugated to alkaline phosphatase were from Bio-Rad Laboratories (Hercules, CA). Horseradish peroxidase-linked goat anti-rabbit IgG, the SuperSignal Ultra chemiluminescent substrate kit, and the Aminolink affinity column were from Pierce (Rockford, IL). Immobilon-P membranes were from Millipore (Bedford, MA). ELISA plates were from Costar

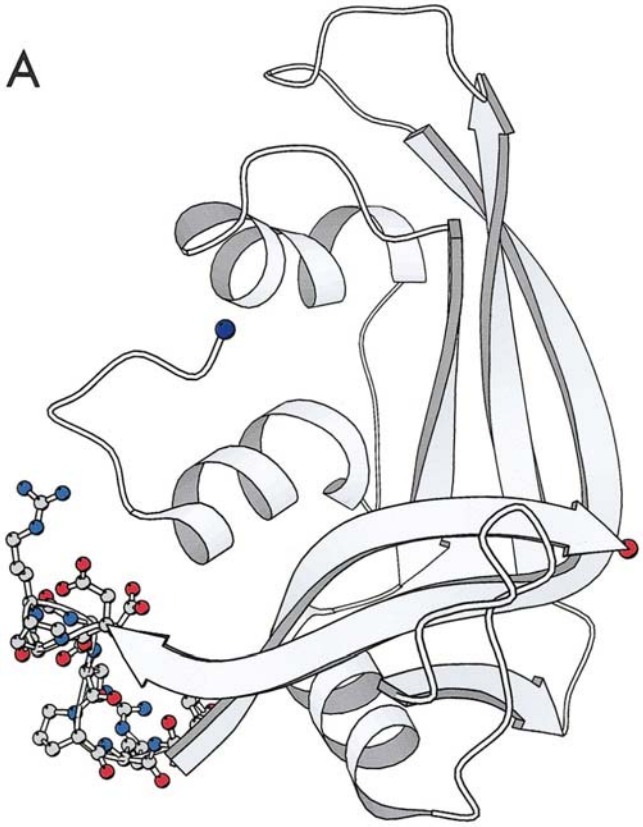

Fig. 1. (A) Ribbon schematic representation of the three-dimensional structure of ECP [16] using the program Molscript [31]. All nonhydrogen atoms are shown for residues D115–Y122. The structure of the loop used as epitope and also the N- and C-terminal ends are shown in color. (B) Amino acid sequence alignment for ECP and its human homologues of the pancreatic RNase family, RNase 1 (pancreatic RNase), EDN (RNase 2), ECP (RNase 3), RNase 4, Ang (RNase 5), and RNase K6 (RNase 6). The alignment was performed with the PileUp program (version 8, Wisconsin Package; Genetics Computer Group). The numbering corresponds to the human ECP sequence. Conserved residues in all the sequences are marked in white with a black background, and conserved residues on either five and four of the sequences are marked in white with a dark-gray background and in black with a light-gray background respectively. The potential glycosylation sites are indicated with arrows. The selected epitope region is indicated with asterisks.

B

```
                    10        20                30        40        50        60
ECP      :  RPPQFTRAQWFAIQHISLNPPR------CTIAMRAINNYRWRCKNQNTFLRTTFANVVNVCGNQSIRCPHNR  :  66
EDN      :  KPPQFTWAQWFETQHINMTSQQ------CTNAMQVINNYQRRCKNQNTFLLTTFANVVNVCGNPNMTCPSNK  :  66
RNaseK6  :  WPKRLTKAHWFEIQHIQPSPLQ------CNRAMSGINNYTQHCKHQNTFLHDSFQNVAAVCDLLSIVCKNRR  :  66
RNase1   :  ---KESRAKKFQRQHMDSDSSPSSSSTYCNQMMRRRNMTQGRCKPVNTFVHEPLVDVQNVCFQEKVTCKNGQ  :  69
RNase4   :  ---QDGMYQRFLRQHVHPE-ETGGSDRYCNLMMQRRKMTLYHCKRFNTFIHEDIWNIRSICSTTNIQCKNGK  :  68
Ang      :  --QDNSRYTHFLTQHYDAKPQ-GRDDRYCESIMRRRGLT-SPCKDINTFIHGNKRSIKAIC--ENKNGNPHR  :  66

                    70        80        90        100       110       120       130
ECP      :  TLNNCHRSRFRVPLLHCDLINPGAQNISNCRYADRPGRRFYVVACDNRD-PRDSPRYPVVPVHLDTTI----  :  133
EDN      :  TRKNCHHSGSQVPLIHCNLTTPSPQNISNCRYAQTPANMFYIVACDNRDQRRDPPQYPVVPVHLDRII----  :  134
RNaseK6  :  --HNCHQSSKPVNMTDCRLT---SGKYPQCRYSAAAQYKFFIVACDPPQ--KSDPPYKLVPVHLDSIL----  :  127
RNase1   :  G--NCYKSNSSMHITDCRLTNGSR--YPNCAYRTSPKERHIIVACEGS----------PYVPVHFDASVEDST  :  128
RNase4   :  M--NCH--EGVVKVTDCRDTGSSR--APNCRYRAIASTRRVVIACEGN----------PQVPVHFDG------  :  119
Ang      :  E--NLRISKSSFQVTTCKLHGGSP--WPPCQYRATAGFRNVVVACENG-----------LPVHLDQSIFRRP  :  123
                                                  *********
```

Corp. (Cambridge, MA). Peptide D112–P123 conjugated with ovalbumin was synthesized and purified by high-pressure liquid chromatography by Neosystem Laboratoire (Strasbourg, France).

Peptide sequence design

The peptide for immunization was selected by comparison of the primary sequences of both human ECP and EDN in the primate family [15] and by comparison of eosinophil-associated RNases ECP and EDN with other members of the pancreatic RNase superfamily [17]. Superposition of the main chain backbone of the human ECP primary sequence on the EDN three-dimensional structure [13] and structure prediction indicated that the loop region corresponding to D115–Y122 is the region where the main chain backbones of the two proteins differ most [14]. Indeed, the sequence corresponds to an exposed loop in the ECP three-dimensional structure—as confirmed recently by X-ray crystallography [16] (Fig. 1A)—containing a unique insertion found in eosinophil RNases (EDN and ECP) and in the phylogenetically close relative RNase K6 (Fig. 1B). A homology search in the protein data bank by the BLAST program (version 8, Wisconsin Package; Genetics Computer Group, Madison, WI) indicated that the selected region has significant homology only with other mammalian ECP sequences [15].

The selected peptide sequence used for immunization (KGDNRDPRDSPRYP) included the loop 115–122 and some extra residues at both sides of the ECP primary sequence (D112–P123). Finally, the KG dipeptide was added at the N terminus, and this K residue was linked to a carrier protein (ovalbumin) to increase the immunogenic response.

Antibody production and partial purification using protein A-Sepharose

The synthetic peptide (KGDNRDPRDSPRYP) conjugated to a carrier protein (ovalbumin) was used as an immunogen, and rabbit polyclonal antibodies were obtained by Neosystem Laboratoire according to their standard immunization protocol. Total antibodies were purified from plasma by means of protein A-Sepharose CL 6B chromatography on a 2-mL column. The column was equilibrated with 50 mM Tris-HCl, pH 7.0, and 2 mL of rabbit serum were run twice through the column. Antibodies were eluted with 0.1 M glycine, pH 3.0; 1 M Tris-HCl, pH 8.0, was added to the collected fractions to neutralize the pH.

Antibody purification by column affinity chromatography with immobilized ECP

rECP, previously obtained in our laboratory using a prokaryotic expression system [14], was used as antigen for the purification of specific antibodies. Following the manufacturer's recommendations, 2 mg of rECP and a 2-mL Aminolink were both equilibrated with phosphate-buffered saline (PBS; 7.5 mM Na_2HPO_4, 2.5 mM NaH_2PO_4, 0.14 M NaCl, pH 7.2). Forty microliters of 5 M sodium cyanoborate were added as a reducing agent, and the mixture was left at 25°C for 6 h and then washed with PBS. Free reactive groups were then blocked with 1 M Tris-HCl, pH 7.4, and the column was washed with 1 M NaCl and equilibrated again in PBS. Two milliliters of immunized rabbit serum were applied to the affinity column, and the column was washed again with PBS and 1 M NaCl. Bound antibodies were eluted with 0.1 M glycine, pH 3.0, and mixed with 1 M Tris-HCl, pH 8.0, to neutralize the pH. Elution was monitored by measuring the absorbance at 280 nm (A_{280}). Peak fractions were pooled, and the final antibody concentration was determined spectrophotometrically ($A_{280}^{0.1\%} = 0.75$). The purified fraction of epitope-specific antibodies was ~10% of the protein A-Sepharose-derived total antibodies.

Preparation of granulocytes

Blood samples were collected from healthy volunteers. Five milliliters of blood samples were mixed with 0.5 mL of 5% EDTA, and 1.375 mL of 3.7% dextran (average relative molecular weight, ~250,000) was added. After a 20-min incubation (37°C) at a 45° inclination and 5 min in a vertical position, the leukocyte-rich plasma fraction was separated and diluted with PBS (1:1, v/v); and then the sample was poured over a Lymphoprep solution (3:1, v/v). After centrifugation of the samples at 800 *g* for 30 min, four layers were formed. The upper plasma fraction was decanted and kept at −20°C until analysis. The pellet, which contained erythrocytes and granulocytes, was further processed as follows. Red blood cells were lysed by adding 0.4 M NH_4Cl to the tubes, which were kept at 0°C for 5 min. The remaining granulocytes were washed twice with PBS, sonicated, and centrifuged before analysis.

Partial purification of plasma by ion-exchange chromatography

Plasma was desalted by gel filtration chromatography with a PD10 column previously equilibrated in a pH 8.0 solution consisting of 15 mM Tris-HCl and 2 mM EDTA. Samples were then loaded onto a HiTrap Q anion-exchange prepacked column that had been equilibrated with 15 mM Tris-HCl–2 mM EDTA, pH 8.0. The nonretained fraction, which contained plasma basic proteins, was loaded onto a cation-exchange column (HiTrap SP) equilibrated in the same buffer. Proteins retained by the cation-exchange column were then eluted with a linear salt gradient of 0–1 M NaCl. Aliquots (0.5 mL) were collected, and the peak fractions were further concentrated and dialyzed against distilled water. Eluted fractions were assayed for activity with zymogram staining gels and were characterized by immunoblotting.

Sputum processing

Healthy volunteers and asthmatic patients were induced to produce sputum via hypertonic saline inhalation. The sputum samples were processed as described by Gibson et al. [18] with the following modifications: sputum plugs were isolated from the sample, diluted (1:4, v/v) with 0.1% dithiothreitol, mixed by vortexing, and kept at room temperature for 15 min to disperse the cells. The samples were diluted 1:4 with PBS, filtered through a 50-μm nylon mesh filter, and centrifuged at 4°C for 10 min at 700 *g*. The supernatant was removed, stored at −20°C, and thawed immediately before assay. The samples were concentrated if necessary and dialyzed against distilled water. The ECP levels in sputum were found to be stable during sputum processing and storage [18].

ELISA

The reactivity of D112–P123 Ab against both the original synthetic peptide conjugated to ovalbumin and rECP was tested by ELISA [19]. The ELISA method was as follows. Wells were coated overnight at room temperature with 100 μL of antigen at different concentrations in a 0.1 M carbonate-bicarbonate buffer, pH 9.6. Wells were washed three times with 0.05% (v/v) Tween 20 in PBS and blocked with 1% bovine serum albumin (BSA) in 0.05% Tween 20 in PBS for 1 h at 37°C. The wells were washed again with the same solution and incubated at 37°C for 2 h with 100 μL of the purified D112–P123 Ab (20 ng/mL–5 μg/mL concentration range) in 1% BSA and 0.05% Tween 20 in PBS. After the wells were washed with 0.05% Tween 20 in PBS, 100 μL of a 1:3,000 dilution of horseradish peroxidase-linked goat anti-rabbit IgG in PBS–1% BSA–0.05% Tween 20 were added per well. Finally, after the wells were washed again with 0.05% Tween 20 in PBS, 100 μL of substrate solution containing 40 mM 3-dimethylaminobenzoic acid, 0.8 mM 3-methyl-2-benzothiazoline hidrazone, and 3 mM H_2O_2 in 0.1 M phosphate buffer, pH 7.0, were added to each well. After a 20-min incubation, the reaction was stopped with 50 μL of 2 M H_2SO_4. The A_{620} was measured with a plate reader (Anthos reader 2001, Anthos Labtec Instruments, Cultek, Spain).

Immunoblotting analysis: Western blot and dot blot

Samples were mixed with loading buffer [60 mM Tris-HCl, 10% (v/v) glycerol, 0.015% (w/v) bromophenol blue, 3% SDS, pH 6.8, with or without 5% β-mercaptoethanol] and loaded onto an SDS–15% polyacrylamide gel. After electrophoresis, proteins were transferred to a prewetted Immobilon P membrane using an optimized transfer buffer for highly cationic proteins [39 mM glycine, 0.1% (w/v) SDS, 20% (v/v) methanol, pH 9.0]. The transfer was performed at 100 V for 25 min. The Immobilon P membranes were washed with Tris-buffered saline (TBS) (25 mM Tris-HCl, 140 mM NaCl, 3 mM KCl, pH 8.0) and blocked with blocking buffer [TBS containing 0.05% Tween 20 and 3% (w/v) BSA]. Detection was carried out with purified D112–P123 Ab as the primary antibody, and the optimal dilution from an initial stock solution of 0.1 mg/mL was previously assessed. Blots were then incubated with the secondary antibody in TBS containing 0.05% Tween 20 and 1% (w/v) BSA, using a

1:3,000 dilution of the biotinylated goat anti-rabbit IgG antibody and a 1:3,000 dilution of the streptavidin-biotinylated alkaline phosphatase complex. Blots were finally developed in a pH 9.5 solution consisting of 100 mM Tris-HCl and 0.5 mM $MgCl_2$ and containing 0.1 mg/mL of 5-bromo-4-chloro-3-indolyl phosphate and 0.3 mg/mL of nitroblue tetrazolium. The reaction was stopped by adding distilled water. Alternatively, blot membranes were developed with a SuperSignal Ultra chemiluminescence kit, using a 1:200,000 dilution of the horseradish peroxidase-linked goat anti-rabbit IgG antibody and the fluorescent substrate luminol. Bands were detected as film signals (Hyperfilm-MP high-performance autoradiography film). For the testing of the monoclonal antibody EG1, a 1:20 dilution was used; and detection was carried out by using a 1:3,000 dilution of alkaline phosphatase-labeled goat anti-mouse antibody. In all cases, bands were scanned (Imaging Densitometer, model GS-700; Bio-Rad Laboratories) and quantified using the software Multi Analyst (version 1.1) (Bio-Rad Laboratories).

For comparison with immunoblotting results, total protein staining was performed with Coomassie blue R-250 dye in 7% acetic acid and 12% methanol. The destaining solution was 7% acetic acid and 20% methanol.

The dot blotting was performed on nitrocellulose membranes with a blotting instrument connected to a vacuum pump (Bio-Dot Microfiltration Apparatus, Bio-Rad Laboratories). Antigen samples were mixed with transfer buffer (39 mM glycine, 0.1% SDS, 20% methanol, pH 9.0) and transferred onto a nitrocellulose membrane. Immunodetection was carried out using purified D112–P123 Ab as the primary antibody and the biotinylated goat anti-rabbit IgG as the secondary antibody according to the procedure described above.

Activity-staining gels (zymogram)

Samples obtained from the partial purification of human plasma and from granulocytes and sputum fractions were mixed with nonreducing loading buffer (60 mM Tris-HCl, 10% glycerol, 0.015% bromophenol blue, 3% SDS, pH 6.8) and were analyzed for RNase activity by zymogram on SDS–15% polyacrylamide gels containing 0.6 mg/mL of either poly(U) or poly(C) as substrate [20]. After elimination of SDS by incubation with a pH 7.5 solution consisting of 10 mM Tris-HCl and 20% isopropanol, the gels were incubated at 25°C for 90 min in 100 mM Tris-HCl, pH 7.5. The gels were stained with 0.2% toluidine blue in 10 mM Tris-HCl, pH 8.0. The relative intensity of the areas showing substrate degradation was analyzed by densitometry.

RESULTS

Purification of D112–P123 Ab by affinity column chromatography

Two milligrams of rECP were immobilized in a 2-mL Aminolink column as described in Materials and Methods. Of the loaded protein, 80–90% was bound to the column. By using this affinity column with immobilized rECP as an antigen, 2 mL of purified antibodies (0.1-mg/mL solutions) were obtained from each 2-mL sample of rabbit serum. The epitope-specific antibody constituted ~10% of the total antibody fraction previously obtained by the protein A-Sepharose chromatography.

Antibody titration and cross-reactivity

Purified antibodies were assayed by ELISA against the conjugated synthetic peptide (0.1–9 μg) and rECP (0.2–37 μg). The antibodies were serially diluted from a 0.1-mg/mL stock solution to working concentrations ranging from 20 ng/mL to 5 μg/mL and added to microtiter plates coated with either rECP or the conjugated peptide. The amount of antibody binding was measured colorimetrically at 620 nm (**Fig. 2**).

Immunoblotting analysis

The immunoreactivity and sensitivity of D112–P123 Ab were first tested against rECP. Immunodetection was carried out after SDS–15% PAGE and transfer to Immobilon membranes. The staining by the streptavidin-biotinylated alkaline phosphatase complex showed that there was a linear relationship for up to ~75 ng of rECP (**Fig. 3A**) and that the assay could detect as little as 1 ng of rECP (Fig. 3B). To check the reproducibility of the method, the relationship between the ECP level (in nanograms) and the integration of the corresponding band densitogram (in optical density units per square millimeter) was obtained from four independent experiments, and the regression line was determined ($y = 0.0755x$; $r^2 = 0.9999$). Immunodetection with a SuperSignal Ultra chemiluminescence kit gave similar results (Fig. 3C), although an increase in the detection levels could be achieved with longer film exposure times. A faint upper band corresponding to the formation of small amounts of dimer was observed when large quantities of purified rECP were loaded on the SDS-polyacrylamide gel. This band was also observed when the SDS-polyacrylamide gel was stained with Coomassie blue for detection of total protein. Lack of cross-reactivity against 3 μg of EDN and RNase A was demonstrated by SDS–15% PAGE and Western blot analysis (**Fig. 4A**).

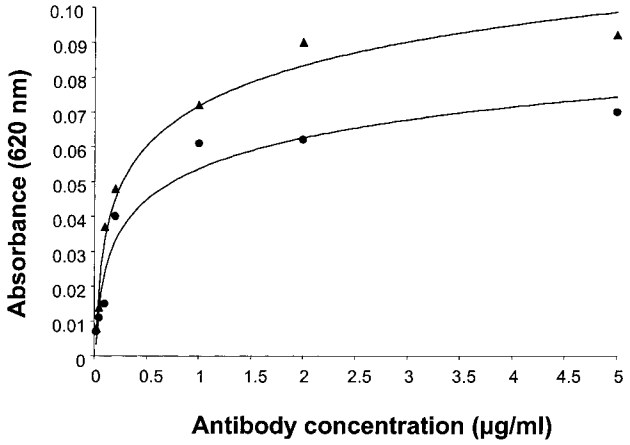

Fig. 2. Analysis of the antibody working range. The relationship between the D112–P123 Ab concentration and the detection signal (A_{620}) using rECP (●) and the conjugated peptide (▲) is shown. The analysis was carried out with the ELISA, using as the secondary antibody the horseradish peroxidase-linked goat anti-rabbit IgG at a 1:3,000 dilution. Solutions of D112–P123 Ab purified by affinity chromatography with immobilized rECP were made ranging from 20 ng/mL to 5 μg/mL, and 200 ng (127 nM) of rECP and 100 ng (19.5 nM) of the conjugated peptide were used as antigens.

D112–P123 Ab reactivity against rECP, the conjugated peptide, and control proteins (0.1–3 μg of EDN, RNase A, and carbonic anhydrase) was also assessed by dot blot analysis. The primary antibody was tested at concentrations ranging from 50 ng/mL to 1 μg /mL, and rECP was tested at concentrations ranging from 1–100 ng. The optimal antibody concentration was 0.2 μg/mL, and rECP was detected down to 10 ng. No signal was detected with either EDN, RNase A, or carbonic anhydrase (results not shown).

To check D112–P123 Ab recognition capability in cells and biological fluids, samples of plasma, granulocytes, and sputum were also assayed by Western blotting and immunodetection (Fig. 4B). In both sputum and granulocyte fractions, we could

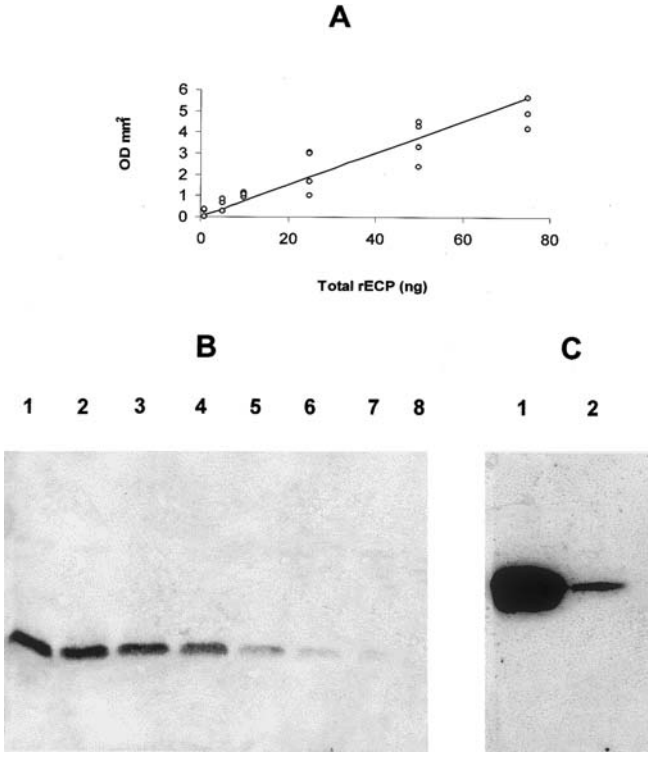

Fig. 3. Analysis of D112–P123 Ab immunoreactivity by Western blot analysis using rECP as antigen. (A) Relationship between rECP (ng) and integrated densitogram of the detected band. After SDS–15% PAGE, the Western blot was developed with the primary antibody D112–P123 Ab at 0.2 μg/mL using biotinylated goat anti-rabbit IgG Ab at a 1:3,000 dilution and streptavidin-biotinylated alkaline phosphatase complex at a 1:3,000 dilution. For each quantity of rECP, four independent measurements were made, and the regression line was determined ($y = 0.0755x$; $r^2 = 0.9999$). (B) SDS–15% PAGE and Western blot analysis developed by the streptavidin-biotinylated alkaline phosphatase complex. Lane 1, 100 ng of rECP; lane 2, 75 ng of rECP; lane 3, 50 ng of rECP; lane 4, 25 ng of rECP; lane 5, 10 ng of rECP; lane 6, 5 ng of rECP; lane 7, 1 ng of rECP; and lane 8, 0.5 ng of rECP. (C) SDS–15% PAGE and Western blot analysis of rECP developed using the SuperSignal Ultra chemiluminescence kit, luminol as substrate, and horseradish peroxidase goat anti-rabbit IgG secondary antibody diluted to 1:200,000. Lane 1, 50 ng of rECP; lane 2, 10 ng of rECP.

identify a lower and predominant band corresponding to the nonglycosylated form, with a molecular mass equivalent to that of rECP. For plasma samples, only the nonglycosylated band was detected.

Plasma samples

For plasma samples, detection of ECP in Western blotting was feasible only if plasma was previously concentrated. ECP levels in serum ranged from ~1 to 20 μg/L in healthy subjects, increasing up to 200–500 μg/L in subjects with inflammatory diseases [2, 15]. Sensitivity was increased by partially purifying plasma samples by ion-exchange chromatography as described in Materials and Methods. SDS-PAGE and total protein staining with Coomassie blue indicated that most of the plasma proteins had been eliminated during the partial purification of the sample (results not shown), although different bands with RNase activity were observed by the zymogram technique (**Fig. 5B**, lane 2). After SDS-PAGE and Western blotting of plasma samples and immunodetection with the streptavidin-biotinylated alkaline phosphatase complex, only a band corresponding to the nonglycosylated form of ECP was detected in the maximum of the elution peak (Fig. 4B, lane 3). This was likely due to the low concentration of ECP in plasma within the limits of the sensitivity of the assay. However, in the initial fraction of the elution peak of ECP from ion-exchange chromatography, two additional bands of 25 and 50 kDa were detected (Fig. 4B, lane 2). The molecular mass of each band was estimated by comparison with standard molecular mass markers. These bands were also detected when the Western blot development was performed without the primary ECP-specific antibody, using only the commercial anti-rabbit IgG secondary antibody (Fig. 4B, lane 6). These bands may correspond to the light and heavy chains of human IgG. Transfer to an Immobilon membrane and N-terminal sequencing of these bands showed that the 25-kDa band corresponded to the light chain of human IgG. In the case of the 50-kDa band, the sequence of the heavy chain was not obtained, probably due to blocking of the N terminus of the protein. N-terminal sequencing indicated the presence of albumin or apolipoprotein H. In conclusion, the bands, identified as human IgG, eluted from the cation ex-

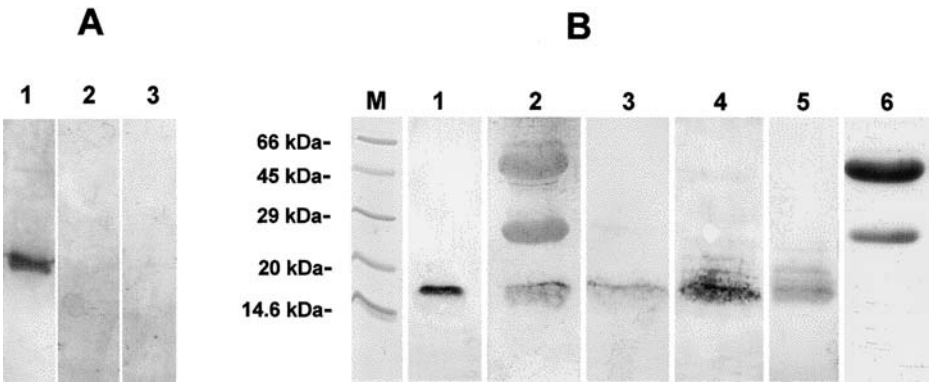

Fig. 4. SDS–15% PAGE and Western blot of rECP and ECP in biological samples. Given the different ECP level in each biological sample, volumes were adjusted to obtain the best detection signal. The primary antibody, D112–P123 Ab, was used at a concentration of 0.2 μg/mL. Blots were developed using biotinylated goat anti-rabbit IgG Ab at a 1:3,000 dilution and streptavidin-biotinylated alkaline phosphatase complex at a 1:3,000 dilution (except in lanes M and 6 of panel B). (A) Lane 1, 50 ng of rECP; lane 2, 3 μg of RNase A; lane 3, 3 μg of EDN. (B) Molecular mass markers stained with Coomassie blue R-250 (bovine serum albumin, ovalbumin, carbonic anhydrase, trypsin inhibitor, and lysozyme). Lane 1, 50 ng of rECP; lane 2, 17 μL of the initial fraction of the ECP elution peak from HiTrap SP chromatography; lane 3, 17 μL of the maximum of the ECP elution peak from HiTrap SP chromatography; lane 4, 15 μL of processed sputum, corresponding to 0.5 mL of initial collected sputum; lane 5, 8 μL of purified granulocytes from 120 μL of total blood; and lane 6, 17 μL of the same sample that was used in lane 2, the incubation step with D112–P123 Ab was omitted, and the blot was developed using a SuperSignal Ultra chemiluminescence kit.

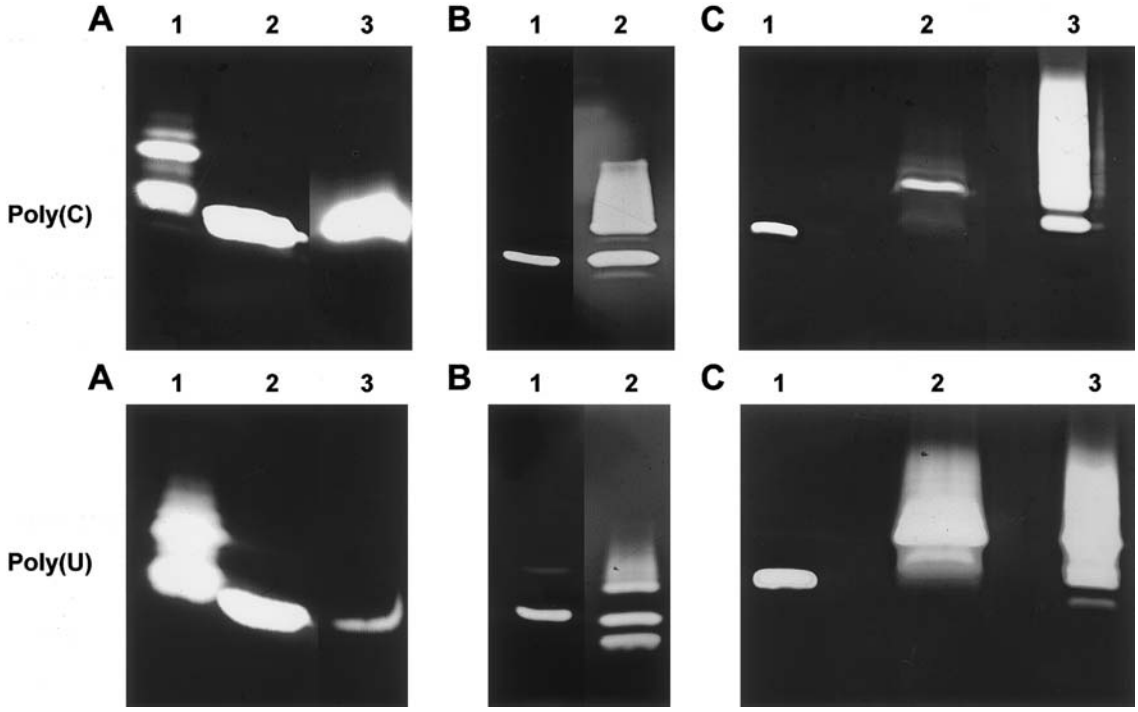

Fig. 5. RNase activity staining on SDS–15% polyacrylamide gels containing either poly(C) (top) or poly(U) (bottom) as substrate. Because the detection signal depends on both the amount of protein and the specific activity of each RNase species, the volumes loaded were accordingly adjusted to obtain the best detection signal. (A) Lane 1, 10 ng of native EDN; lane 2, 170 ng of rECP; lane 3, 150 pg of RNase A. (B) Lane 1, 100 ng of rECP; lane 2, 5 μL of HiTrap SP peak fraction. (C) Lane 1, 100 ng of rECP; lane 2, 6 μL of purified granulocytes corresponding to a volume of 60 μL of total blood; lane 3, 3 μL of processed sputum, corresponding to 0.1 mL of initial collected sputum. The differences in the activities of ECP bands depended on the incubation times.

change column at high ionic strength, close to the maximum peak fraction for ECP, during the partial purification from plasma and did not cross-react with the ECP-specific primary antibody.

Granulocyte samples

Three glycosylated forms of native ECP, with approximate molecular masses of 18, 20, and 22 kDa, have been described in the literature [7, 8]. In the granulocyte samples, we detected a lower band with a molecular mass corresponding to the nonglycosylated rECP and some additional bands of higher molecular mass, which could be attributed to glycosylated forms of ECP (Fig. 4B, lane 5). In this case, only one RNase activity band was detected with poly(C) as the substrate; but several bands were observed with poly(U) (Fig. 5C, lane 2).

The ECP content in granulocytes includes the quantities detected in eosinophils, neutrophils, and basophils. Granulocytes are mainly composed of neutrophils (95.8%) but also contain smaller proportions of eosinophils (3.5%) and basophils (0.6%), with the ECP content of neutrophils being 30- to 100-fold lower than that of the eosinophils [21, 22]. Abughazaleh et al. [21] reported ECP concentrations of ~5 $\mu g/10^6$ cells in eosinophils, 50 $ng/10^6$ cells in neutrophils, and 80 $ng/10^6$ cells in basophils; and recent immunofluorescence studies indicated ECP contents of ~3.4 $\mu g/10^6$ cells in eosinophils and 150 $ng/10^6$ cells in neutrophils [22]. Very recent studies suggest that the ECP content detected in neutrophils results from an active uptake by the neutrophils of the protein secreted by the eosinophils [2].

Sputum samples

Sputum analysis is one of the selective noninvasive markers of airway inflammation. Measurement of ECP levels in sputum seems to reflect inflammation and bronchial obstruction better than that of ECP levels in blood [23]. Processing of sputum samples was carried out as described in Material and Methods. Treatment with 0.1% dithiothreitol ensures cell dispersion, and the assayed fraction corresponds to the sputum supernatant [18]. The sputum supernatant reflects only the ECP released by eosinophil degranulation, although the possibility of a small percentage of eosinophil lysis due to sample handling cannot be ruled out. Western blot analysis allows detection of a predominantly nonglycosylated band as well as some additional bands of higher molecular mass in the sputum supernatant (Fig. 4B, lane 4), although a more detailed study is necessary to quantify and identify the different glycosylated forms. ECP reference values in the literature range from 20- to 600-μg/L; values of >400–600 μg/L are found in asthmatic patients [18]. RNase activity was also analyzed by the zymogram technique (Fig. 5C, lane 3).

We used the sputum samples to check the recognition capability of D112–P123 Ab in relation to the values determined by the UniCAP™ system. Both systems yielded comparable results (**Table 1**). The Western blot method was used to determine the ECP levels and the relationship between the integrated densitogram of each band, and the ECP quantity was correlated using the regression line obtained from Figure 3A ($y = 0.0755x$; $r^2 = 0.9999$). In each assay, an rECP sample

TABLE 1. Determination of ECP Levels in Sputum Samples by Immunoreactivity of the D112–P123 Ab and by the UniCAP™ System

Sample[a]	ECP level (μg/L) by D112–P123 Ab[b]	ECP level (μg/L) by UniCap™ system
1	301	368
2	1,495	1,248
3	382	312
4	ND[c]	112

[a] Samples were obtained from volunteers. Sample 1 corresponds to a healthy volunteer and samples 2 through 4 correspond to treated asthmatic patients. [b] ECP levels were determined by Western blot analysis from the bands detected by the D112–P123 Ab. The ECP values were obtained by integration of the band densitograms and interpolation using the regression line obtained as shown in Fig. 3. In each assay an rECP sample (75 ng) was used as internal standard. [c] ND: not detected.

(75 ng) was used as an internal standard. Treated asthmatic patients showed control values, except in case number 2; these samples were used only as a reference to compare the two methods.

Activity-staining analysis

Samples of partially purified plasma, granulocytes, and sputum were also analyzed for RNase activity by the activity-staining method (zymogram) using poly(C) and poly(U) as substrates. Both ECP and EDN belong to the pancreatic RNase family [17] and have RNase activity. Up to now, six different RNases have been detected in human body fluids and characterized [17] (Fig. 1B). The proteins with RNase activity—which elute from the cation-exchange chromatography equilibrated with 15 mM Tris-HCl, pH 8.0, at NaCl concentrations from 0.1 to 0.5 M—are the basic RNases, which include pancreatic RNase (RNase 1), EDN (RNase 2) , ECP (RNase 3), RNase 4, angiogenin (RNase 5), and RNase K6 (RNase 6) (Fig. 1B). Several glycosylated forms have been described for the human pancreatic RNase [24] and the eosinophil RNases [17]. Comparative activity staining with both poly(C) and poly(U) substrates was used for the qualitative differential analysis of plasma RNases [19]. Quantitative analysis of the bands detected by activity staining cannot be performed because several RNases and their glycosylated forms have similar molecular masses. Furthermore, the relative catalytic efficiency of the different glycosylated isoforms for the polynucleotide substrates is not yet known.

RNase A, EDN, and ECP show different cleavage rates for the poly(U) and poly(C) substrates (Fig. 5A). While pancreatic RNase 1 shows a preference for the poly(C) substrate, eosinophil RNases prefer poly(U), although the poly(U)/poly(C) ratio is much higher for EDN than for ECP. The zymogram is a very sensitive technique that can detect as little as 50–100 pg of RNase A [29], 1–5 ng of native EDN [19], and 10–15 ng of rECP [14]. In Figures 5B and C, the bands detected by poly(U) and poly(C) activity-staining electrophoresis of granulocytes, plasma, and sputum samples are compared. Comparison of the plasma fraction (Fig. 5B, lane 2) with the granulocyte sample (Fig. 5C, lane 2) shows a predominance of eosinophil RNases in the granulocyte fraction, with a clear preference for poly(U).

DISCUSSION

ECP levels in biological fluids have been correlated to the severity of asthma and other chronic inflammatory diseases in which a specific degranulation of the eosinophil is observed during the inflammation process [2]. However, there is some controversy regarding the clinical diagnostic usefulness of ECP levels in some fluids and tissues because of either the sample handling protocols [25, 26] or the detection assay specificity [27].

We have developed an epitope-specific polyclonal antibody for the specific immunodetection of ECP. A specific epitope was selected according to a prediction of ECP's three-dimensional structure [13]. The region that corresponds to an exposed loop in ECP, where the main chain adopts a different conformation in EDN than in ECP, was selected. The recently resolved crystal structure of ECP [16] confirmed the chosen region as a putative antigenic epitope (Fig. 1A).

Polyclonal antibodies were raised using a conjugated synthetic peptide corresponding to the sequence D112–P123, which includes the identified loop region D115–Y122. Specific purification of the antibodies on an affinity column using immobilized rECP as an antigen eliminated any possible background due to the rabbit immunogenic reaction to the carrier protein or to any other secondary structure adopted by the synthetic peptide that did not correspond to its conformation in the three-dimensional native structure.

D112–P123 Ab reacted with the nonglycosylated rECP, expressed in a prokaryote system, and with the native human ECP present in plasma, granulocytes, and sputum. In the Western blot, a lower band corresponding to the nonglycosylated protein and additional bands of higher molecular mass, which would correspond to the ECP glycosylated forms, were detected by the antibody. The antibody had a high sensitivity, detecting as little as 1 ng of rECP; it could detect ECP in both its reduced and nonreduced forms, and this antibody did not cross-react with either EDN or RNase A.

Immunoblotting results were always compared with those obtained by Coomassie blue total protein staining and by the zymogram technique. The activity-staining method had a very high sensitivity but could not discriminate between the different proteins with RNase activity and similar molecular masses or between the corresponding glycosylated isoforms present in biological samples.

D112–P123 Ab recognition capability can be compared with that of other ECP immunodetection assays. However, both the source of the antigen and the antibody specificity have to be taken into account. Monoclonal antibodies EG1 and EG2 raised against eosinophil extracts and eosinophil granule products [9] have been suggested to be useful for the monitoring of eosinophil degranulation. EG1 recognizes ECP in both its storage and secreted forms, and EG2 recognizes both ECP and EDN, albeit only in their secreted forms. EG1 can be used only in nonreducing conditions, and EG2 detects only one glycosylated form of ECP [7]. Detection with EG2 has been used in

many clinical studies as a tool to distinguish between resting and actively secreting eosinophils, and such a method is useful for monitoring and diagnosing inflammatory diseases. However, the physiological significance of stored and secreted forms of eosinophil RNases is still controversial, and the structural differences are unknown. Moreover, Jahnsen et al. [28] have shown that the EG2 reactivity does not discriminate between resting and activated eosinophils. These authors concluded that EG2 antibody could not be used as an activation marker in immunohistochemistry. Their results suggested that the reported differences in staining were likely caused by the granule protein leaking from the eosinophils as a result of the fixation technique rather than as a result of cellular secretion. Recently, Nakajima et al. [27] tested the EG1 and EG2 reactivity by radioimmunoassay and Western blot analysis and concluded that their differential reactivity was dependent on both the method of fixation and the antibody concentration.

We have compared the binding affinities and specificities of D112–P123 Ab and EG1. Immunoblotting in nonreducing conditions using a 1:10 dilution of EG1 antibody could detect rECP as well as plasma and granulocyte ECP; there was no cross-reaction with other proteins, but there was a slightly lower sensitivity than that of D112–P123 Ab at a 1:500 dilution. Some basic research studies have also been carried out using polyclonal antibodies against purified native ECP [10, 29].

Most of the current clinical studies use the newly developed Pharmacia CAP System™ for the monitoring of ECP levels, with a detection limit of ~2 ng/mL [11]. Unfortunately, there is not much literature available on either its specificity or the epitope recognized by the antibody. In sputum samples, a good correlation has been obtained between the automated assay of the Pharmacia CAP System™ (UniCAP™) and D112–P123 Ab recognition (Table 1).

D112–P123 Ab should prove useful for the analysis of different ECP isoforms in biological tissues and fluids. The antibody does not cross-react with EDN, can be used in both reducing and nonreducing conditions, and has a sensitivity detection limit of 1 ng. In the present study, a preliminary analysis of ECP isoforms in plasma, granulocytes, and sputum samples was carried out using the ECP epitope-specific D112–P123 Ab. Further analyses will be carried out to characterize and quantify the glycosylated forms of ECP in plasma, eosinophils, and sputum. It has been reported that the several ECP isoforms display different biological properties [2]. Glycosylation is regarded as a way of fine-tuning to modulate the functionality of the secreted protein and as a target-cell recognition marker [30]. The specific identification and quantification of the ECP glycosylated forms will help us understand the process of ECP secretion and regulation. To assess the putative involvement of this domain in ECP biological properties, functional studies of the neutralizing effects of the epitope-specific D112–P123 Ab will also be performed.

ACKNOWLEDGMENTS

This work was supported by grants PB96-1172-C02-01 from the Dirección General de Enseñanza Superior of the Ministerio de Educación y Cultura (Spain) and SGR98-00065 from Comissió Interdepartmental de Ciència i Tecnologia of the Generalitat de Catalunya. Esther Carreras was a recipient of a predoctoral fellowship grant from Universitat Autònoma de Barcelona.

The authors are grateful to Dr. Franchek Drobnic (Centre d'Alt Rendiment Esportiu, Sant Cugat del Vallès, Spain) for providing blood and sputum samples and for his advice on the sample processing protocols and to Dr. José Belda (Servei de Pneumologia, Hospital de la Santa Creu i Sant Pau, Barcelona, Spain) for providing sputum samples and for determining the ECP levels using the UniCap™ system. We thank Dr. G. J. Gleich (Department of Immunology, Mayo Clinic and Mayo Foundation, Rochester, MN) for providing native EDN. We also thank Dámaso Torres for his contribution to the ICM modeling of ECP, Dr. K. R. Acharya for his help in the analysis of the X-ray crystal structure of ECP, and Dr. Gennady Moiseyev for helpful discussions.

REFERENCES

1. Rosenberg, H. F., Ackerman, S. J., Tenen, D. G. (1989) Human eosinophil cationic protein—molecular cloning of a cytotoxin and helminthotoxin with ribonuclease-activity. J. Exp. Med. 170, 163–176.
2. Venge, P., Bystrom, J., Carlson, M., Hakansson, L., Karawacjzyk, M., Peterson, C., Seveus, L., Trulson, A. (1999) Eosinophil cationic protein (ECP): molecular and biological properties and the use of ECP as a marker of eosinophil activation in disease. Clin. Exp. Allergy 29, 1172–1186.
3. Olszewska Pazdrak, B., Pazdrak, K., Ogra, P. L., Garofalo, R. P. (1998) Respiratory syncytial virus—infected pulmonary epithelial cells induce eosinophil degranulation by a CD18-mediated mechanism. J. Immunol. 160, 4889–4895.
4. Harrison, A. M., Bonville, C. A., Rosenberg, H. F., Domachowske, J. B. (1999) Respiratory syncytial virus-induced chemokine expression in the lower airways. Am. J. Resp. Crit. Care Med. 159, 1918–1924.
5. Takafuji, S., Tadokoro, K., Ito, K., Nakagawa, T. (1998) Release of granule proteins from human eosinophils stimulated with mast-cell mediators. Allergy 53, 951–956.
6. Kato, K., Fujisawa, T., Terada, A., Iguchi, K. (1999) Mechanism of eosinophil cationic protein release in the serum: role of adhesion molecules. Int. Arch. Allergy Immunol. 120, 60–64.
7. Rosenberg, H. F., Tiffany, H. L. (1994) Characterization of the eosinophil granule proteins recognized by the activation-specific antibody EG2. J. Leukoc. Biol. 56, 502–506.
8. Peterson, C. G. B., Jornvall, H., Venge, P. (1988) Purification and characterization of eosinophil cationic protein from normal human eosinophils. Eur. J. Haematol. 40, 415–423.
9. Tai, P. C., Spry, C. J. F., Peterson, C., Venge, P., Olsson, I. (1984) Monoclonal antibodies distinguish between storage and secreted forms of eosinophil cationic protein. Nature 309, 182–184.
10. Reimert, C. M., Venge, P., Kharazmi, A., Bendtzen, K. (1991) Detection of eosinophil cationic protein (ECP) by an enzyme-linked-immunosorbent-assay. J. Immunol. Methods 138, 285–290.
11. Zimmerman, B., Lanner, A., Enander, I., Zimmerman, R. S., Peterson, C. G. B., Ahlstedt, S. (1993) Total blood eosinophils, serum eosinophil cationic protein and eosinophil protein-X in childhood asthma—relation to disease status and therapy. Clin. Exp. Allergy 23, 564–570.
12. Yman, L., Ewan, P., deGroot, H., Lange, C., Lindholm, N., Paganelli, R., Roovers, M., Sastre, J. (1996) Clinical efficiency of UniCAP™ specific IgE. J. Allergy Clin. Immunol. 97, 208.
13. Boix, E., Nikolovski, Z., Moiseyev, G. P., Rosenberg, H. F., Cuchillo, C. M., Nogués, M. V. (1999) Kinetic and product distribution analysis of human eosinophil cationic protein indicates a subsite arrangement that favors exonuclease-type activity. J. Biol. Chem. 274, 15605–15614.
14. Mosimann, S. C., Newton, D. L., Youle, R. J., James, M. N. G. (1996) X-ray crystallographic structure of recombinant eosinophil-derived neurotoxin at 1.83 Å resolution. J. Mol. Biol. 260, 540–552.

15. Rosenberg, H. F., Dyer, K. D., Tiffany, H. L., González, M. (1995) Rapid evolution of a unique family of primate ribonuclease genes. Nat. Genet. 10, 219–223.
16. Boix, E., Leonidas, D. D., Nikolovski, Z., Nogués, M. V., Cuchillo, C. M., Acharya, K. R. (1999) Crystal structure of eosinophil cationic protein at 2.4 Å resolution. Biochemistry 38, 16794–16801.
17. Zhang, J. Z., Rosenberg, H. F., Nei, M. (1998) Positive Darwinian selection after gene duplication in primate ribonuclease genes. Proc. Natl. Acad. Sci. USA 95, 3708–3713.
18. Gibson, P. G., Woolley, K. L., Carty, K., Murree Allen, K., Saltos, N. (1998) Induced sputum eosinophil cationic protein (ECP) measurement in asthma and chronic obstructive airway disease (COAD). Clin. Exp. Allergy 28, 1081–1088.
19. Bravo, M. I., Cuchillo, C. M., Nogués, M. V. (1995) Identification of human nonpancreatic-type ribonuclease by antibodies obtained against a synthetic peptide. Biol. Chem. Hoppe-Seyler 376, 555–560.
20. Bravo, J., Fernández, E., Ribó, M., De Llorens, R., Cuchillo, C. M. (1994) A versatile negative-staining ribonuclease zymogram. Anal. Biochem. 219, 82–86.
21. Abughazaleh, R. I., Dunnette, S. L., Loegering, D. A., Checkel, J. L., Kita, H., Thomas, L. L., Gleich, G. J. (1992) Eosinophil granule proteins in peripheral-blood granulocytes. J. Leukoc. Biol. 52, 611–618.
22. Sur, S., Glitz, D. G., Kita, H., Kujawa, S. M., Peterson, E. A., Weiler, D. A., Kephart, G. M., Wagner, J. M., George, T. J., Gleich, G. J., Leiferman, K. M. (1998) Localization of eosinophil-derived neurotoxin and eosinophil cationic protein in neutrophilic leukocytes. J. Leukoc. Biol. 63, 715–722.
23. Grebski, E., Wu, J., Wuthrich, B., Medici, T. C. (1999) Does eosinophil cationic protein in sputum and blood reflect bronchial inflammation and obstruction in allergic asthmatics? J. Invest. Allerg. Clin. Immunol. 9, 82–88.
24. Ribó, M., Beintema, J. J., Osset, M., Fernández, E., Bravo, J., De Llorens, R., Cuchillo, C. M. (1994) Heterogeneity in the glycosylation pattern of human pancreatic ribonuclease. Biol. Chem. Hoppe-Seyler 375, 357–363.
25. Reimert, C. M., Poulsen, L. K., Bindslev-Jensen, C., Kharazmi, A., Bendtzen, K. (1993) Measurement of eosinophil cationic protein (ECP) and eosinophil protein X/eosinophil derived neurotoxin (EPX/EDN). J. Immunol. Methods 166, 183–190.
26. Marks, G. B., Kjellerby, J., Łuczynska, C. M., Burney, P. G. J. (1998) Serum eosinophil cationic protein: distribution and reproducibility in a randomly selected sample of men living in rural Norfolk, UK. Clin. Exp. Allergy 28, 1345–1350.
27. Nakajima, H., Loegering, D. A., Kita, H., Kephart, G. M., Gleich, G. J. (1999) Reactivity of monoclonal antibodies EG1 and EG2 with eosinophils and their granule proteins. J. Leukoc. Biol. 66, 447–454.
28. Jahnsen, F. L., Brandtzaeg, P., Halstensen, T. S. (1994) Monoclonal-antibody EG2 does not provide reliable immunohistochemical discrimination between resting and activated eosinophils. J. Immunol. Methods 175, 23–36.
29. Ackerman, S. J. (1993) Characterization and functions of eosinophil granule proteins. In *Eosinophils: Biological and Clinical Aspects* (S. Makino and T. Fukuda, eds.), Boca Raton, FL, CRC Press 33–74.
30. Rudd, P. M., Woods, R. J., Wormald, M. R., Opdenakker, G., Downing, A. K., Campbell, I. D., Dwek, R. A. (1995) The effects of variable glycosylation on the functional activities of ribonuclease, plasminogen and tissue-plasminogen activator. Biochim. Biophys. Acta 1248, 1–10.
31. Kraulis, P. J. (1991) Molscript—a program to produce both detailed and schematic plots of protein structures. J. Appl. Crystallogr. 24, 946–950.

CAPÍTOL 3

Articles

Both Aromatic and Cationic Residues Contribute to the Membrane-Lytic and Bactericidal Activity of Eosinophil Cationic Protein†

Esther Carreras,‡ Ester Boix,‡ Helene F. Rosenberg,§ Claudi M. Cuchillo,‡ and M. Victòria Nogués*,‡

Departament de Bioquímica i Biologia Molecular, Facultat de Ciències, Universitat Autònoma de Barcelona, 08193-Bellaterra, Spain, and Laboratory of Host Defenses, NIAID, National Institutes of Health, Bethesda, Maryland 20892 USA

Received December 4, 2002; Revised Manuscript Received March 7, 2003

ABSTRACT: Eosinophil cationic protein (ECP) and eosinophil derived neurotoxin (EDN) are proteins of the ribonuclease A (RNase A) superfamily that have developed biological properties related to the function of eosinophils. ECP is a potent cytotoxic molecule, and although the mechanism is still unknown this cytotoxic activity has been associated with its highly cationic character. Using liposome vesicles as a model, we have demonstrated that ECP tends to disrupt preferentially acidic membranes. On the basis of structure analysis, ECP variants modified at basic and hydrophobic residues have been constructed. Changes in the leakage of liposome vesicles by these ECP variants have indicated the role of both aromatic and basic specific amino acids in cellular membrane disruption. This is the case with the two tryptophans at positions 10 and 35, but not phenylalanine 76, and the two arginines 101 and 104. The bactericidal activity of both native ECP and point-mutated variants, tested against *Escherichia coli* and *Staphylococcus aureus*, suggests that basic amino acids play, in addition to the effect on the disruption of the cellular membrane, other roles such as specific binding on the surface of the bacteria cell.

Eosinophil cationic protein (ECP)[1] is a secretory protein found in the large specific granules of eosinophilic leukocytes. Mature ECP is a single polypeptide with a molecular mass of 15.5 kDa, although several glycosylated forms with molecular masses ranging from 16 to 22 kDa have also been observed. It shares sequence homology with proteins of the RNase A superfamily, a vertebrate-specific enzyme family (*1*), that includes eight human proteins, with different RNase activities, expression patterns, and physiological functions that, in some cases, remain unknown (*2*). Eosinophils also contain another member of the RNase A superfamily, the eosinophil derived neurotoxin (EDN), that shows a 67% amino acid sequence identity with ECP. ECP shares the overall three-dimensional structure and active site amino acids required for RNase activity (*3*), although its catalytic activity is much lower (*4*, *5*). ECP has developed biological properties, related to the functions of the eosinophils, and the ECP levels in different biological fluids correlate with the eosinophil activity which is used as an inflammatory marker (*6*). ECP is a potent cytotoxic molecule, with bactericidal (*7*, *8*) and helminthotoxic (*9*, *10*) properties in contrast with EDN which has very little antibacterial and antiparasitic activities. The cytotoxic effect of ECP can also damage the host epithelial cells (*11*, *12*). Both ECP and EDN are neurotoxic and provoke the Gordon phenomenon when injected intraventricularly to guinea pig and rabbits (*13*); they also possess antiviral activity against the single-stranded RNA respiratory syncytial virus (RSV) (*14*).

It has been suggested that the pathogenic activity of ECP appeared due to a strong positive Darwinian selection occurring after the duplication of the ancestral EDN gene about 30 million years ago, resulting in an increase of the net positive charge of the protein (*15*, *16*). ECP shows an isoelectric point of 10.8, and its highly cationic character is dependent on the number of arginine residues at the molecular surface which may increase the capacity to bind negatively charged molecules of cellular membranes. The

† This work was supported by Grants 2000SGR-00064 and 2001SGR-00196 from the Direcció General de Recerca of the Generalitat de Catalunya and BMC2000-0138-C02-01 from the Dirección General de Investigación of the Ministerio de Ciencia y Tecnología (Spain). Esther Carreras was a recipient of a predoctoral fellowship from Universitat Autònoma de Barcelona.

* To whom correspondence should be addressed. Phone: 34-93-5811256. Fax: 34-93-5811264. E-mail: victoria.nogues@uab.es.

‡ Universitat Autònoma de Barcelona.

§ National Institutes of Health.

[1] Abbreviations: ECP, eosinophil cationic protein; rECP, recombinant eosinophil cationic protein; wtECP, wild-type eosinophil cationic protein; EDN, eosinophil derived neurotoxin; RSV, respiratory syncytial virus; MBP, major basic protein; (Δ115−122)-ECP, an ECP variant in which the region of the loop D115−Y122 has been deleted; (115−122EDN)-ECP, an ECP variant in which the region of the loop D115−Y122 has been substituted by the corresponding sequence of EDN; $(Up)_4U>p$, an oligouridylic acid of five residues ending in a 2′,3′-cyclic phosphate; poly(U), polyuridylic acid; ANTS, 8-aminonaphthalene-1,3,6-trisulfonic acid disodium salt; DPX, *p*-xylene-bis-pyridinium bromide; DOPC, 1,2-dioleoyl-*sn*-glycero-3-phosphocholine; DOPG, 1,2-dioleoyl-*sn*-glycero-3-[phospho-rac-(1-glycerol)]; SASA, solvent accessible surface area; CFU, colony forming units; rmsd, residue mean standard deviation.

10.1021/bi0273011 CCC: $25.00
Published on Web 05/16/2003

mechanism of cytotoxicity of ECP is still unknown and its relation to the RNase activity is controversial. While the ability of ECP to kill bacteria and parasites does not depend on its ribonucleolytic activity (*8*, *17*), ECP and EDN need the catalytic activity to display their neurotoxicity (*18*) and antiviral activity (*19*). Purified ECP is able to form stable nonion selective channels in cell membranes (*20*). Thus, it is plausible to think that ECP can kill cells by a mechanism similar to that of some other pore-forming proteins such as polymerized C9 (*21*). In addition to the transmembrane pore formation, ECP could penetrate the cell where, like other cytotoxic RNases, the subsequent cleavage of RNA would result eventually in cell death. In these cases, reaching the cell's cytosol is very likely the rate limiting step for its cytotoxic activity. It was shown that the increase of net positive charge of RNase A by chemical modification increases its cytotoxicity probably by enhancing its cellular uptake (*22*). On the other hand, ECP blocks selectively the growth of some mammalian cell lines (*23*). Recently, a new member of the RNase superfamily, named RNase 7, with a high cationicity and a broad antimicrobial spectrum, has been identified in human skin and other tissues (*24*, *25*).

The aim of this work is focused on the amino acid residues of ECP, which may interact with the cell membrane and, hence, be responsible for its toxicity. We have used site-directed mutagenesis to modify some residues and checked the cytotoxicity of the ECP variants obtained. On the basis of the three-dimensional structure of ECP (*3*), we have chosen some cationic and hydrophobic residues from the surface of the protein. In addition, we have studied the role of the loop region 115−122, which is specific for both eosinophil RNases and for RNases 6, 7, and 8 and is one of the regions where ECP and EDN differ the most (Figure 1 A). For each ECP variant, the kinetic parameters for ribonucleolytic activity were measured and compared with those of ECP. In addition to the bactericidal effect on both Gram-negative and Gram-positive bacteria, we have determined the ability of wild-type ECP and ECP variants to disrupt the membranes using liposome vesicles as a model.

EXPERIMENTAL PROCEDURES

Site-Directed Mutagenesis, Expression, and Purification of ECP Variants. All mutants were obtained from a human ECP synthetic gene (*5*). R121A- and W10K-ECP mutants and the construction with the deletion of the region 115−122 ((Δ115−122)-ECP) were constructed using standard PCR techniques (*26*). The double variants R75A/F76A-, R121A/Y122A-, W35A/R36A-, R101A/R104A-ECP, as well as the construction where the 115−122 region of ECP is replaced by the corresponding EDN sequence ((115−122EDN)-ECP), were constructed using the Quick Change Site-Directed Mutagenesis kit (Stratagene, La Jolla, CA). All constructs were confirmed by DNA sequencing.

Protein expression in the *Escherichia coli* BL21(DE3) strain (Novagen, Madison, WI) as well as the initial purification steps and folding of the proteins from inclusion bodies were carried out as previously described (*5*). In the subsequent cationic exchange chromatography (Resource S and Mono S columns, Amersham Pharmacia Biotech) purification steps, the proteins were injected in 0.15 M sodium acetate, pH 5, and eluted with a linear NaCl gradient from 0 to 2 M in the same buffer. Differences in the elution pattern were a consequence of the different net charge of each mutant. The homogeneity of the purified proteins was checked with 15% SDS−PAGE and Coomasie Blue staining and MALDI-TOF mass spectrometry (*5*).

Assay of RNase Activity. The RNase activity of the recombinant proteins was determined using the oligouridylic acid $(Up)_4U>p$ as substrate. This substrate was chosen based on the previous kinetic characterization studies of ECP and was prepared from poly(U) digestion (*5*). Assays were carried out in 50 mM MES−NaOH, pH 6.2, at 25 °C, and the kinetic parameters were determined by the spectrophotometric method using 1-cm path length cells (*5*). Substrate concentration was determined using the extinction coefficient $\epsilon_{260} = 12\,500\ M^{-1}\ cm^{-1}$ (*5*). The activity was measured by following the initial reaction velocities using the difference molar absorbance coefficient, in relation to the cleaved phosphodiester bond ($\Delta\epsilon_{280} = 700\ M^{-1}\ cm^{-1}$). Substrate concentrations ranged from 0.01 to 0.3 mM. Final enzyme concentrations varied between 0.14 and 0.5 μM, depending on the activity of each mutant.

Liposome Leakage as a Measure of Membrane Disruption Capacity. Liposome vesicles were prepared by vacuum-drying of a 1,2-dioleoyl-*sn*-glycero-3-phosphocholine (DOPC)/1,2 dioleoyl-*sn*-glycero-3-[phospho-rac-(1-glycerol)] (DOPG) (3:2 molar ratio) chloroform solution. DOPC and DOPG were from Avanti Polar Lipids. Alternatively, pure DOPG and DOPC vesicles were prepared. To obtain large unilamelar vesicles with incorporated ANTS/DPX, the lipid film was hydrated in 12.5 mM ANTS, 45 mM DPX, 20 mM NaCl, 10 mM Tris, pH 7.5 and mixed overnight in the dark. The suspension was frozen and thawed 20 times in liquid nitrogen. The liposome vesicles were extruded successively through 0.8, 0.4, and 0.1-μm (pore diameter) polycarbonate membranes (Whatman) and centrifuged at 12 000*g* for 10 min to discard nonincorporated lipids. Unencapsulated material was separated from the vesicles by gel filtration on Sephadex G-25 (Amersham Pharmacia Biotech) using 10 mM Tris-HCl, pH 7.5 containing 0.1 M NaCl and 1 mM EDTA as elution buffer. The lipid concentration was determined by a colorimetric assay method for free and phosphorylated glyceric acids (*27*).

Leakage was measured using the 8-aminonaphthalene-1,3,6-trisulfonic acid disodium salt (ANTS)/*p*-xylene-bis-pyridinium bromide (DPX) fluorescence assay (*28*) as described by de los Rios et al. (*29*) with minor modifications. ANTS and DPX were from Molecular Probes. Leakage was measured by fluorescence (Perkin-Elmer 650-4 Fluorescence spectrophotometer). Excitation and emission wavelengths were 386 and 535 nm, respectively. The slit widths were 5 nm for the excitation beam and 10 nm for the emission beam. The percentage of leakage (%*L*) produced by the proteins after 1 h of incubation with the liposomes was calculated with the following equation:

$$(\%L) = 100(F_p - F_o)/(F_{100} - F_o)$$

where F_p is the final fluorescence intensity after addition of the protein (1 h), F_o and F_{100} are the fluorescence intensities before addition of the protein and after addition of 0.5% Triton X100 (Sigma), respectively. Statistical analysis was performed by using the Student's t test. A p value < 0.05 was considered statistically significant.

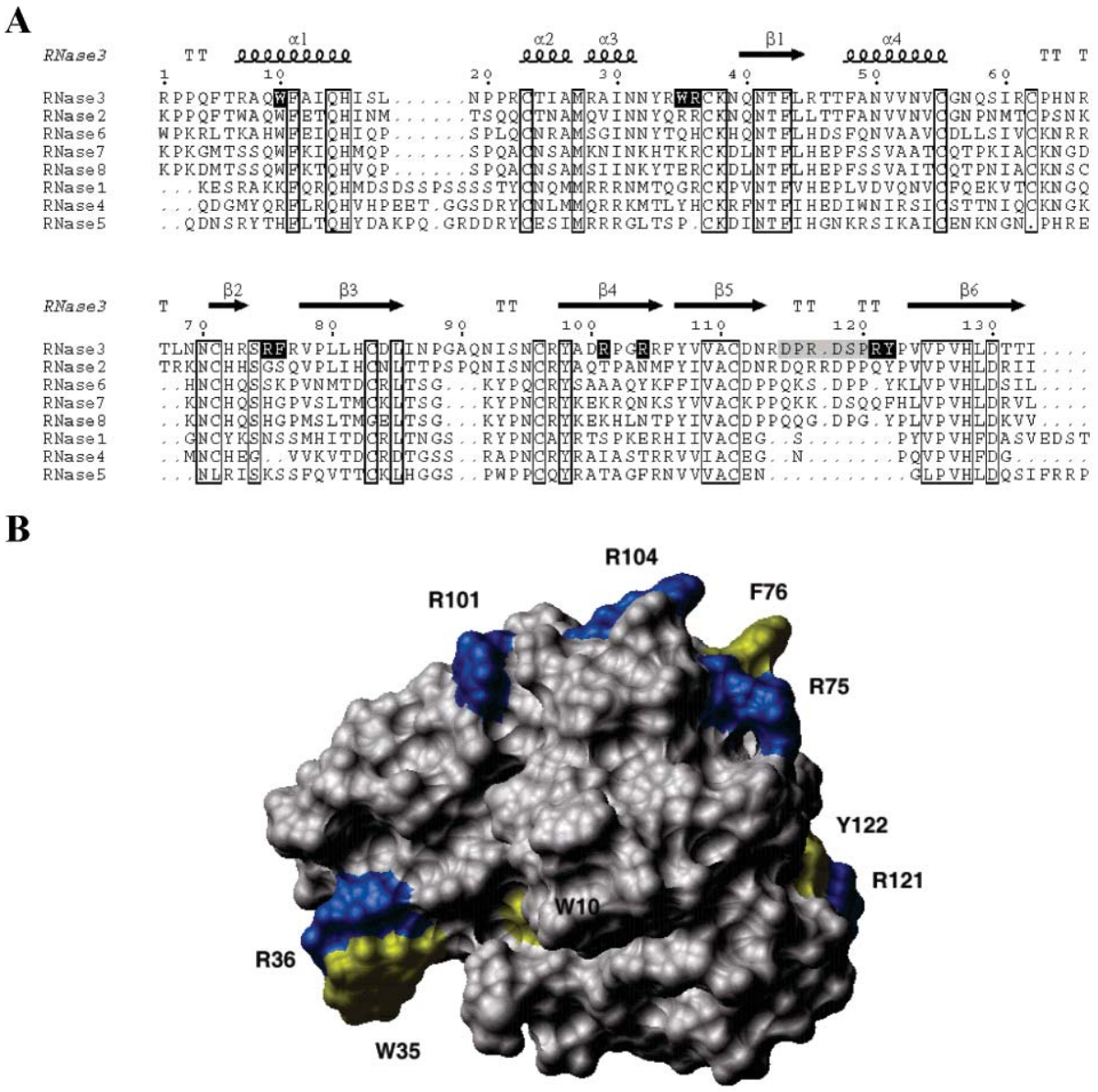

FIGURE 1: Location of the mutated residues on the ECP structure. (A) Primary sequence alignment of human members of the RNase A superfamily. The conserved amino acids are boxed. The selected residues for amino acid substitutions are highlighted in black for single mutation and gray for the loop region. The secondary elements of the ECP structure are shown. The alignment was generated with Clustal W and the picture was drawn using the ESPript program (*43*). (B) Molecular surface representation of the X-ray three-dimensional structure of ECP (1QMT.pdb) showing the position of the mutated residues, with basic amino acid residues (Arg) in blue and hydrophobic residues (Phe, Tyr, and Trp) in yellow. The picture has been drawn using ICM software.

Antibacterial Activity Assay. Antibacterial assay with recombinant proteins was carried out essentially as described by Lehrer et al. (*7*). Overnight cultures of *Escherichia coli* BL21 DE3 strain and *Staphylococcus aureus* 502 A strain (ATCC, Rockville, MD) were washed twice and suspended at 1:100 or 1:1000 with respect to the original volume in 10 mM sodium phosphate, pH 7.5. Aliquots of 20 μL of bacterial suspension were incubated for 4 h at 37 °C with different concentrations (0.5, 1, and 2 μM) of each ECP variant in phosphate buffer or with the same volume of phosphate buffer as a control. The 10-fold dilutions of the treated bacterial suspensions were plated on Luria-Bertani (LB) agar followed by overnight growth at 37 °C, and the colony forming units (CFU)/mL for each treatment was determined. In each experiment, all the assays were carried out in triplicate, and the results obtained were the average of three independent experiments. EDN antibacterial activity was also tested as a negative control. Statistical analysis was performed by using the Student's *t* test. A p value < 0.05 was considered statistically significant. Results were explained in terms of the highest concentration with a significant p value.

The antibacterial activity of recombinant ECP (rECP) at different time intervals between 0 and 4 h was checked on the *E. coli* BL21 DE3 strain by the same procedure using a 2 μM protein concentration.

Molecular Modeling. Three-dimensional models of ECP mutants were obtained based on the X-ray structure of ECP (1QMT·pdb and ref *3*) using the software Internal Coordinate Modeling (ICM, and ref *30*). The solvent accessible surface area (SASA) was calculated using the program MolMol (*31*).

Table 1: Determination of the Total Atomic Charge and Solvent Accessible Surface Area (SASA) Values of Wild-Type and ECP Variants

protein	total atomic charge[a]	% of solvent accessible surface area[b]	total solvent accessible surface area[c]
wild-type ECP	13.73		8196.28
W10K	14.73	9	8207.81
W35A + R36A	12.74	62 + 39	8040.42
R75A + F76A	12.74	53 + 53	8112.36
R101A + R104A	11.75	34 + 47	8098.32
R121A	12.74	56	8016.71
R121A + Y122A	12.74	56 + 20	8118.93
(115−122 EDN)-ECP	13.73		8453.70
(Δ115−122)-ECP	13.75		7857.94

[a] Total atomic charge calculated using the Modeling Software ICM. The electrostatic solvation energy was calculated using the boundary element method (MolSoft and ref *30*). [b] Percent of solvent accessible surface area (SASA) calculated by the MolMol program (*31*), using a solvent radius = 1.4 Å. The values were calculated for the mutated residue in the context of the ECP wild-type surface. Values 0−20% are characteristic of buried residues, 20−40% of partially buried residues, and >40% of surface exposed residues. [c] Total SASA of rECP and the predicted three-dimensional structure of ECP variants calculated using the Modeling Software ICM (MolSoft and ref *30*).

RESULTS

Design and Purification of ECP Mutants. ECP variants were constructed to analyze the contribution of specific basic and aromatic amino acid residues located on the surface of the protein (W10K-, W35A/R36A-, R75A/F76A-, and R101A/R104A-ECP) and at the loop D115−Y122 to the ECP cytotoxic activities (Figure 1). The sequence D115−Y122 of ECP corresponds to a unique exposed region which is a large insertion loop in eosinophil-associated RNases (ECP and EDN) and in RNases 6, 7, and 8. To analyze the role of this region, the following constructions were obtained: the (Δ115−122)-ECP form in which the whole loop was deleted, the (115−122 EDN)-ECP form in which the ECP specific amino acids were substituted by the corresponding EDN residues (116Q/P117R/S120P/R122Q-ECP) and specific variants (R121A-ECP and R121A/Y122-ECP).

The predicted three-dimensional structures of ECP variants using the Internal Coordinate Modeling (ICM, MolSoft) (*31*) did not show any significant deviation from the overall structure of wild-type ECP. The overall residue mean standard deviation (rmsd) of superimposed main chain backbones was in all cases lower than 0.5 Å, except for the form with the EDN loop ((115−122 EDN) ECP), where the loop region has a rmsd around 1.5 Å, and the protein with the deletion of the region D115−Y122 ((Δ115−122)-ECP), where the last five C-terminal residues positions show a shift of about 1.5 Å. All the mutated residues are solvent exposed at the molecule surface, except for W10, which is partly buried and close to the active site cavity. The solvent accessible surface area and the electrostatic potential of the protein show variations depending on the amino acids substitutions (Table 1).

ECP variants obtained by site-directed mutagenesis were purified according to the general procedure described for rECP (*5*), but the steepness of the salt gradient applied to the cation exchange chromatography was optimized in each case. The molecular mass of the purified ECP variants was checked by MALDI-TOF mass spectrometry.

Table 2: Steady-State Kinetic Parameters for the Cleavage of $(Up)_4U>p$ by Wild-Type and ECP Variants[a]

protein	k_{cat} (s^{-1})	K_m (mM)	k_{cat}/K_m (M^{-1} s^{-1})
wild-type ECP	0.68 ± 0.06	0.08 ± 0.01	8500
W10K	0.28 ± 0.03	0.07 ± 0.01	4000
W35A/R36A	1.23 ± 0.10	0.09 ± 0.01	13 700
R75A/F76A	0.31 ± 0.01	0.08 ± 0.01	3900
R101A/R104A	1.54 ± 0.14	0.08 ± 0.01	19 200
R121A	1.00 ± 0.09	0.11 ± 0.02	9000
R121A/Y122A	1.07 ± 0.10	0.10 ± 0.02	10 700
(115−122 EDN)-ECP	1.09 ± 0.10	0.13 ± 0.02	8400
(Δ115−122)-ECP	0.34 ± 0.03	0.06 ± 0.01	5700

[a] The substrate was prepared from poly(U) digestion (*5*). The spectrophotometric method was used. Reaction conditions: 50 mM MES−NaOH, pH 6.2 at 25 °C. Substrate concentration ranges were from 0.01 to 0.3 mM. Final enzyme concentrations were from 0.14 to 0.5 μM depending on the activity of each mutant.

Kinetic Characterization of ECP Variants. Table 2 shows the steady-state kinetic parameters for the cleavage of $(Up)_4U>p$ by rECP and the modified forms. This low molecular weight substrate was chosen according to the previous kinetic characterization of rECP (*5*), which indicated an increase in efficiency for the cleavage of oligouridylic acids $(Up)_nU>p$ from $n = 1$ to $n = 4$. ECP has a RNase activity lower than other members of the RNase A superfamily such as EDN or RNase A and the ECP modified forms of this study showed only slight changes in the kinetic parameters with respect to rECP. The highest increase in the catalytic efficiency is observed for the R101A/R104A variant. This effect may be explained in terms of the role of the positive charges located at the surface of the protein as attractants for the negative groups of the substrate as proposed by Mallorquí-Fernández et al. (*32*). The presence of the positive charges might hinder the access of the substrate to the active site or produce a modification of the active site through an indirect effect.

Leakage Capacity on Liposome Vesicles. Lehrer et al. (*7*) analyzed the bactericidal activity of ECP against *E. coli* and *S. aureus* and its effect on the integrity of the bacterial outer and inner membranes of *E. coli*. To further understand the molecular basis of the ECP bactericidal activity (*7*, *8*), we have analyzed the membrane disruptive capacity of the ECP variants with the aim of clarifying the relationship between the cytotoxic activity of ECP and the effect on membrane stability. Lipid vesicles have proven to be a good model to analyze the ECP effect on cellular membranes. Using DOPC/DOPG (3:2 molar ratio) vesicles, a 1.5 μM concentration of ECP produces a leakage of 50% of the total, while the 100% value is obtained at 5 μM (Figure 2A). These protein concentrations correspond to a vesicle/protein molar ratio of 23 and 7, respectively. No detectable effect was observed under the same conditions for both EDN and RNase A with protein concentrations up to 5 μM. These results demonstrate the specific effect of ECP on the membrane's stability. We also analyzed the effect of the net charge of the lipid vesicles on the membrane permeability produced by ECP (Figure 2B) and showed that this effect depends on the presence of negative charges on the synthetic membranes. These results suggest that ECP cytotoxicity may be mediated by the disruption of the cell membrane integrity and that the electrostatic interactions between the negative charges of the membranes and specific positive charges on the protein surface are crucial for its membrane disruptive capacity.

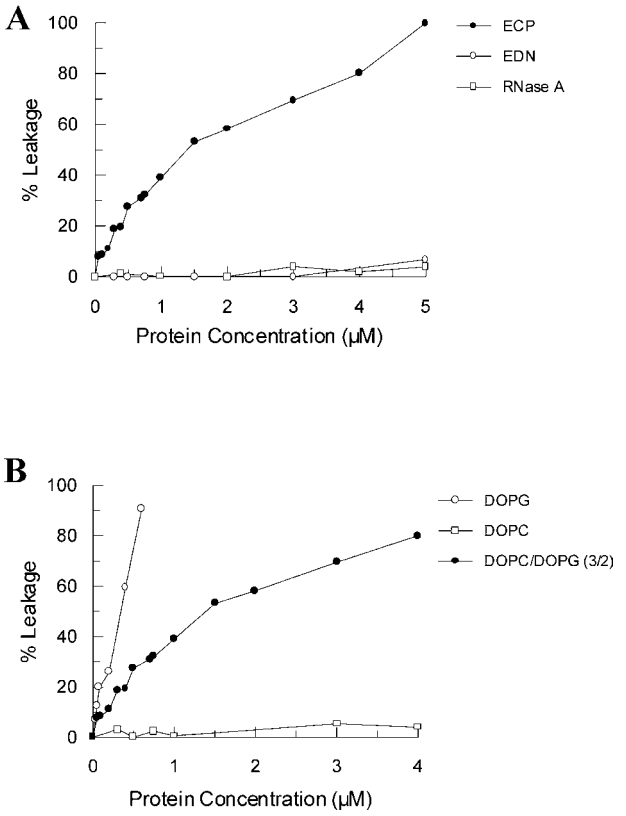

FIGURE 2: Effect of ECP, EDN, and RNase A in the leakage capacity on liposome vesicles. (A) Effect of ECP, EDN, and RNase A on the ANTS/DPX leakage from DOPC and DOPG (3:2 molar ratio) vesicles. (B) Leakage induced by ECP on vesicles containing different proportions of DOPC/DOPG. Only DOPG (○), DOPC/DOPG (3:2 molar ratio) (●) and only DOPC (□).

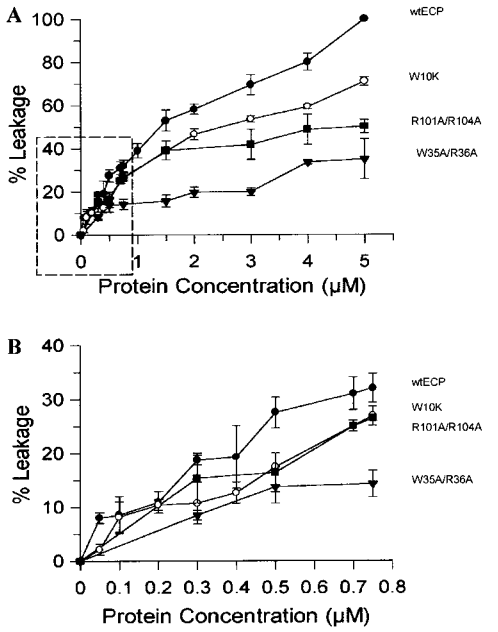

FIGURE 3: Effect of ECP variants which show a significant decrease in the leakage capacity on liposome vesicles compared to the effect of wild-type. (A) Percentage of leakage of W10K-, W35A/R36A-, and R101A/R104A- and wtECP. The effect was analyzed in the leakage of DOPC/DOPG (3/2 molar ratio) vesicles. Statistical significance of the decrease in the percentage of leakage with respect to ECP: $p < 0.01$ for W35A/R36A-ECP, $p < 0.05$ for W10K-ECP (in both cases for all protein concentrations tested) and $p < 0.05$ for R101A/R104A-ECP (for most protein concentrations). (B) Detail of the boxed region in panel A.

We analyzed therefore the effect of the ECP variants modified at specific basic and hydrophobic amino acid residues on the leakage capacity of liposome vesicles. Our results indicate that the observed effect is dependent on the specific amino acid location and not only on the overall net charge or the hydrophobic character of the variant. W35A/R36A-, R101A/R104A-, and W10K-ECP are the variants that cause a significant decrease on the leakage capacity of the liposome vesicles (Figure 3). The effect observed in the W10K-ECP variant demonstrates the role of hydrophobic amino acids without removal of any cationic residue. On the other hand, not every cationic residue is equally important: the leakage is modified in the R101A/R104A variant but not from alterations in R121 or R75. Statistical significance for the decrease in the percentage of leakage of mutants with respect to ECP was $p < 0.01$ for W35A/R36A-ECP, $p < 0.05$ for W10K-ECP (in both cases for all protein concentrations tested), and $p < 0.05$ for R101A/R104A-ECP (for most of protein concentrations). No changes in leakage with respect to ECP was observed for the other mutants (results not shown).

Bactericidal Activity of ECP and ECP Variants. The bactericidal activity of ECP against *E. coli* and *S. aureus* and the effect of different factors as incubation time, protein concentration, temperature, and pH was described by Lehrer et al. (*7*). Figure 4 A shows the kinetics of bactericidal activity of rECP against *E. coli*. The profile of CFU/mL versus incubation time is similar to that of native ECP purified from eosinophils (*7*). This profile indicates that the ECP effect is of a bactericidal nature, although a simultaneous bacteriostatic activity cannot be discarded. Figure 4B,C shows the effect in the bactericidal activity of wild-type and variants of ECP against Gram-negative (*E. coli* BL21 DE3) and Gram-positive (*S. aureus* 502A) strains, expressed as CFU/mL remaining after exposure to different protein concentrations. ECP concentrations up to 2 μM reduce significantly the CFU/mL values of both *E. coli* and *S. aureus*, as previously reported Lehrer et al. (*7*) and Rosenberg (*8*). EDN concentrations up to 2 μM were also tested. No effect was observed (data not shown) in agreement with previous results (*8*).

Figure 4B shows the toxicity of ECP variants with changes in the region corresponding to the loop 115−122 compared to the control. This loop is specific for both human eosinophil RNases and RNases 6, 7, and 8 (Figure 1A) (*2*). A decrease in the CFU/mL value is observed for the variants (Δ115−122)-ECP ($p < 0.02$), R121A- and R12A/Y122A-ECP in Gram-positive bacteria. These variants show a similar effect to that of rECP on the tested Gram-negative bacteria. Figure 4C includes the effect produced by modified forms of ECP which alter specific amino acid residues located on the surface of the protein. W35A/R36A-ECP substitutions decrease the CFU/mL value of ECP for both Gram-negative ($p < 0.02$) and Gram-positive ($p < 0.01$) bacteria. Selective toxicity is found for the other variants studied. W10K-ECP decreases the cytotoxicity of ECP against *S. aureus* ($p < 0.001$), while R101A/R104A-ECP ($p < 0.05$) and R75A/F76A-ECP ($p < 0.01$) reduce the toxicity against *E. coli*. Comparison of Figures 3 and 4 indicates that the bactericidal

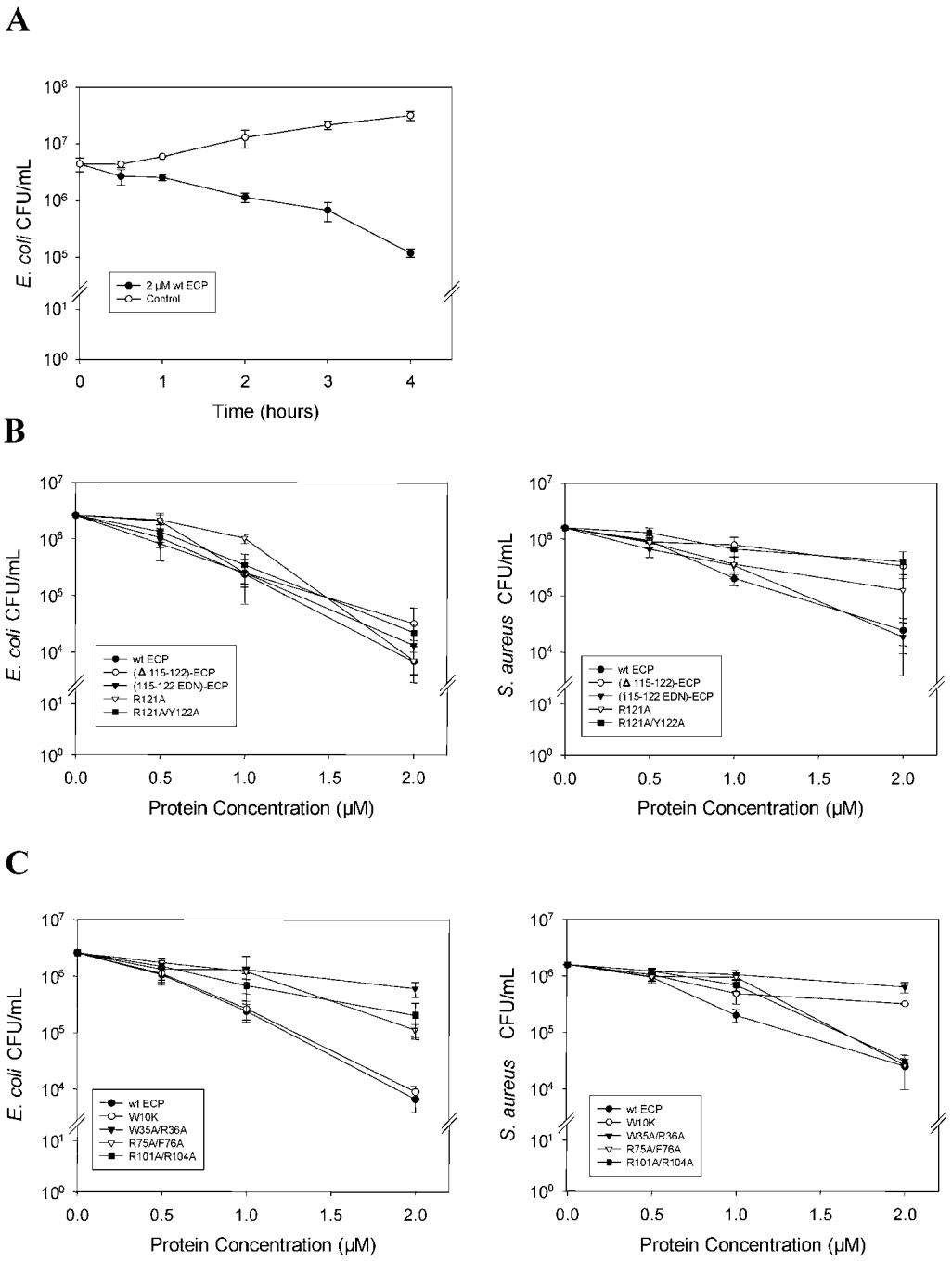

FIGURE 4: Bactericidal activity of wild-type and ECP variants against *S. aureus* and *E. coli*, expressed as percentage of CFU/mL remaining after exposure to different protein concentrations. (A) Kinetics of bactericidal activity of rECP (2 μM) against *E. coli*. (B) Effect of amino acid residues located at the loop D115−Y122. (C) Effect of changes in amino acid residues located on the protein surface. *S. aureus* or *E. coli* cultures in stationary phase were incubated with 0.5, 1, and 2 μM concentration of specific ECP samples or with the same volume of buffer control for 5 h at 37 °C. Statistical significance: $p < 0.02$ for W35A/R36A-, $p < 0.05$ for R101/R104-, and $p < 0.01$ for R75A/F76A-ECP for the bactericidal activity against *E. coli* with respect to ECP and $p < 0.01$ for W35A/R36A-, $p < 0.001$ for W10K-, and $p < 0.02$ for (Δ115−122)-ECP against *S. aureus*.

activity does not correlate well with the leakage capacity on liposome vesicles. The relationship between the bactericidal activity, the structural characteristics, and possible functions of the modified amino acids of each variant is analyzed in the discussion section.

DISCUSSION

It had been proposed that the bactericidal activity of ECP, which is not observed in other proteins of the RNase superfamily such as EDN or RNase A, is a consequence of the high number of arginine residues on the molecular surface (*3*). The overall surface charge for ECP is 14, in contrast to the values of 7 and 3 for EDN and RNase A, respectively (*3*). However, a potential role for hydrophobic residues cannot be excluded. We have constructed mutants that modify specific basic and aromatic amino acid residues located in the D115−Y122 loop and on the surface of the protein with the aim of analyzing the molecular basis of this

activity. The variants were selected from comparison of the sequence and three-dimensional superposition of both ECP and EDN. Residues only present in the ECP structure were considered as potentially important for the bactericidal activity (Figure 1A). We also centered the analysis on the regions with the highest potential for interaction with the cell membrane and on the most exposed positive and hydrophobic residues on the surface of the protein (Figure 1B). Therefore, we constructed variants that modify the loop 115−122, by deletion of the sequence 115−122 ((Δ115−122)-ECP form), by substitution of ECP specific amino acids for the corresponding EDN residues (−116Q/P117R/S120P/R122Q-ECP) ((115−122 EDN)-ECP form) and specific variants of this region (R121A-, R121A/Y122-ECP). Variants that alter the hydrophobic and/or basic character of the protein surface as W10K-, W35A/R36A-, R75A/F76A-, and R101A/R104A-ECP were also constructed. ECP has its only two tryptophan residues at positions 10 and 35. W35 is specific for ECP in the RNase A superfamily and in the ECP structure is the most exposed surface residue, and its change to alanine modifies considerably the solvent accessible surface area (Table 1). In the W35A/R36A-ECP variant, the adjacent arginine residue (R36) was also changed to alanine to eliminate the corresponding contribution of the electrostatic interaction of the region. Tryptophan in position 10 is specific for eosinophil RNases and is less exposed to the solvent than W35 (Figure 1B). We changed tryptophan 10 to lysine to mimic an RNase key residue (K7) involved both in substrate binding and catalytic activity (*33*). Finally, the substituted basic amino acids (R75, R101, and R104) have their side chain exposed to the solvent and, together with F76, form a cluster involved in the crystal packing of ECP (*3*).

ECP shows a low RNase activity in comparison with EDN or RNase A, and previous studies by Rosenberg (*8*) showed that the ECP bactericidal activity was maintained in mutants where the RNase activity had been abolished. Our results indicate that the amino acid changes introduced in our variants do not modify substantially the RNase kinetic parameters (Table 2) except for the R101A/R104A and W35A/R36A variants that showed an increase in activity. However, in the two latter cases, a decrease in the bactericidal activity against *E. coli* (Figure 4) and in the leakage capacity on liposome vesicles (Figure 3) were also observed. These results suggest that the changes in the RNase activity are not directly correlated with the bactericidal activity. A recent study on the cationization of both RNase A and human RNase 1 has concluded that the increase in the protein net charge facilitates their cellular uptake. In that case, contrary to the case of ECP, catalytic activity is required for the cytotoxicity to malignant cell lines (*22*).

We have demonstrated that ECP, in contrast to EDN and RNase A, is able to permeate liposome vesicles, and that the net charge of the lipid vesicles is crucial for its action (Figure 2). Besides, differences dependent on the analyzed bacterial strains suggest that selective structural features of the protein are involved in the binding and disruption capacities of ECP to particular bacterial cell walls and membranes.

While mutants W35A/R36A-, R101A/R104A-, and W10K-ECP have shown a decrease in the bactericidal activity, at least in one of the tested bacterial strains, in parallel with the decrease in the leakage of liposome vesicles with respect to wild-type (Figure 3), R75A/F76A- and (Δ115−122)-ECP mutants show a reduced bactericidal activity which does not correlate with a decrease in leakage activity. Studies of antimicrobial peptides indicate that tryptophan prefers lipid−water interfaces, while phenylalanine, with its nonpolar aromatic ring, is mostly located in the core of the membrane (*34*−*36*). Our results point out the importance of specific aromatic residues in the process: tryptophan, but not phenylalanine substitution, reduces liposome leakage. The effect on the decrease of leakage of liposome vesicles in the case of the R101A/R104A- variant may be associated with the strong electrostatic interaction that may take place in the wild-type ECP (wtECP) between the positive charges in the side chains of these very close arginine residues and the negative groups of DOPG lipids. Our results indicate that ECP destabilizes preferentially acidic liposome vesicles (Figure 2). Major basic protein (MBP), another eosinophil granule protein with a very high isoelectric point (pI $\approx$ 11), which contains alternating hydrophobic and cationic residues, mainly interacts with anionic lipid vesicles, inducing their aggregation and lysis (*37*). Dathe et al. (*38*) have analyzed the destabilization of liposome vesicles by peptides and have observed that the most active peptides against negatively charged bilayers, such as we have demonstrated for ECP, accumulate on the surface of the membrane without deep insertion into the acyl chain region because of electrostatic binding in the lipid headgroup region.

The bactericidal activity of proteins may be due to a particular binding or other specific effect on the surface of the bacterial cell, depending on whether it is a Gram-positive or Gram-negative species. The polypeptides may bind to Gram-negative bacteria through electrostatic interactions with the negatively charged lipopolysaccharide, the major component of the outer leaflet of the outer membrane, followed by insertion into the lipid matrix. After crossing the peptidoglycan layer, the protein, ECP in this case, could bind to the negatively charged groups of the cytoplasmic membrane, bring about its destabilization through hydrophobic interactions, and translocate across the bilayer (*38*). Lehrer et al. (*7*) have demonstrated that ECP and MBP produce a decrease in the colony count in parallel with the permeabilization of the outer and inner membranes of *E. coli*. In the case of Gram-positive bacteria, the negative charge on the surface is provided by the teichoic acids of the cell wall. Before interacting with the negatively charged cytoplasmic membrane, the protein should have to cross first the thick peptidoglycan barrier, and then, the effects on the cytoplasmic membrane might be similar to those described for Gram-negative bacteria. In both cases, two types of specific interactions are necessary: on one hand, the electrostatic binding between the negative groups of the membrane and basic amino acids of the protein and, on the other hand, specific hydrophobic interactions involved in membrane disruption. However, the hydrophobic and electrostatic binding energies of proteins at the membrane interfaces are not just additive; in fact, the hydrophobic free energy reduces the effective valence of cationic peptides (*39*). In this context, the studied amino acids may play different roles in the ECP bactericidal activity. Those changes that only modify the level of bactericidal activity but do not cause liposome vesicle leakage (R75A/F76A- and (Δ115−122)-ECP) could

correspond to residues involved in the binding processes between the protein and the bacteria. In contrast, amino acid substitutions that alter liposome vesicles leakage may be associated with effects on membrane destabilization (W10K-, W35A/R36A-, R101A/R104A-ECP). No clear relationship between membrane disruption and bactericidal activity has also been reported in the case of many cationic antimicrobial peptides (*40*, *41*).

In conclusion, the studied amino acids play different roles in the bactericidal activity of ECP. The modified residues in the variants that selectively modify the level of bactericidal activity or the liposome vesicle leakage, may be involved in the different steps of the bactericidal process. We are planning to further characterize the ECP binding to bacteria and the membrane disruption process, as well as other potential steps in the protein bactericidal mechanism. Bactericidal proteins and peptides constitute a first immune defense barrier (*42*). The understanding of the molecular basis of the antimicrobial activity of proteins and peptides involved in the host immune defense offers an alternative strategy to antibiotic development.

ACKNOWLEDGMENT

The authors are grateful to Dámaso Torres (Departament de Bioquímica i Biologia Molecular, Universitat Autònoma de Barcelona) for molecular modeling with ICM software and to Dr. Ramon Barnades (Departament de Bioquímica i Biologia Molecular, Universitat Autònoma de Barcelona) for the technical support in the studies with liposome vesicles.

REFERENCES

1. Beintema, J. J., Schüller, C., Irie, M., and Carsana, A. (1988) Molecular evolution of the ribonuclease superfamily. *Prog. Biophys. Mol. Biol. 51*, 165−192.
2. Zhang, J., Dyer, K. D., and Rosenberg, H. F. (2002) RNase 8, a novel RNase A superfamily ribonuclease expressed uniquely in placenta. *Nucleic Acids Res. 30*, 1169−1175.
3. Boix, E., Leonidas, D. D., Nikolovski, Z., Nogués, M. V., Cuchillo, C. M., and Acharya, K. R. (1999) Crystal structure of eosinophil cationic protein at 2.4 Å resolution. *Biochemistry 38*, 16794−16801.
4. Slifman, N. R., Loegering, D. A., McKean, D. J., and Glich, G. J. (1986) Ribonuclease activity associated with human eosinophil-derived neurotoxin and eosinophil cationic protein. *J. Immunol. 137*, 2913−2917.
5. Boix, E., Nikolovski, Z., Moiseyev, G. P., Rosenberg, H. F., Cuchillo, C. M., and Nogués, M. V. (1999) Kinetic and product distribution analysis of human eosinophil cationic protein indicates a subsite arrangement that favors exonuclease-type activity. *J. Biol. Chem. 274*, 15605−15614.
6. Venge, P., Byström, J., Carlson, M., Hakansson, L., Karawacjzyk, M., Peterson, C., Sevéus, L., and Trulson, A. (1999) Eosinophil cationic protein (ECP): molecular and biological properties and the use of ECP as a marker of eosinophil activation in disease. *Clin. Exp. Allergy 29*, 1172−1186.
7. Lehrer, R. I., Szklarek, D., Barton, A., Ganz, T., Hamann, K. J., and Gleich, G. J. (1989) Antibacterial properties of eosinophil major basic protein and eosinophil cationic protein. *J. Immunol. 142*, 4428−4434.
8. Rosenberg, H. F. (1995) Recombinant human eosinophil cationic protein ribonuclease activity is not essential for cytotoxicity. *J. Biol. Chem. 270*, 7876−7881.
9. McLaren, D. J., McKean, J. R., Olsson, I., Venge, P., and Kay, A. B. (1981) Morphological studies on the killing of schistosomula of *Schistosoma mansoni* by human eosinophil and neutrophil cationic proteins *in vitro*. *Parasite Immunol. 3*, 359−373.
10. Ackerman, S. J., Gleich, G. J., Loegering, D. A., Richardson, B. A., and Butterworth, A. E. (1985) Comparative toxicity of purified human eosinophil granule cationic proteins for schistosomula of *Schistosoma mansoni*. *Am. J. Trop. Med. Hyg. 34*, 735−745.
11. Motojima, S., Frigas, E., Loegering, D. A., and Gleich, G. J. (1989) Toxicity of eosinophil cationic proteins for guinea pig tracheal epithelium in vitro. *Am. Rev. Respir. Dis. 139*, 801−805.
12. Tai, P. C., Ackerman, S. J., Spry, C. J., Dunnette, S., Olsen, E. G., and Gleich, G. J. (1987) Deposits of eosinophil granule proteins in cardiac tissues of patients with eosinophilic endomyocardial disease. *Lancet 1*, 643−647.
13. Fredens, K., Dahl, R., and Venge, P. (1982) The Gordon phenomenon induced by the eosinophil cationic protein and eosinophil protein X. *J. Allergy Clin. Immunol. 70*, 361−366.
14. Domachowske, J. B., Dyer, K. D., Adams, A. G., Leto, T. L., and Rosenberg, H. F. (1998) Eosinophil cationic protein/RNase 3 is another RNase A-family ribonuclease with direct antiviral activity. *Nucleic Acids. Res. 26*, 3358−3363.
15. Rosenberg, H. F., Dyer, K. D., Lee, T. H., and Gonzalez, M. (1995) Rapid evolution of a unique family of primate ribonuclease genes. *Nat. Genet. 10*, 219−223.
16. Zhang, J., Rosenberg, H. F., and Nei, M. (1998) Positive Darwinian selection after gene duplication in primate ribonuclease genes. *Proc. Natl. Acad. Sci. U.S.A. 95*, 3708−3713.
17. Molina, H. A., Kierszenbaum, F., Hamann, K. J., and Gleich, G. J. (1988) Toxic effects produced or mediated by human eosinophil granule components on *Trypanosoma cruzy*. *Am. J. Trop. Hyg. Med. 38*, 327−334.
18. Sorrentino, S., Glitz, D. G., Hamann, K. J., Loegering, D. A., Checkel, J. L., and Gleich, G. J. (1992) Eosinophil-derived neurotoxin and human liver ribonuclease. Identity of structure and linkage of neurotoxicity to nuclease activity. *J. Biol. Chem. 267*, 14859−14865.
19. Domachowske, J. B., and Rosenberg, H. F. (1997) Eosinophil inhibit retroviral transduction of human target cells by a ribonuclease-dependent mechanism. *J. Leukocyte Biol. 62*, 363−368.
20. Young, J. D.-E., Peterson, C. G. B., Venge, P., and Cohn, Z. A. (1986) Mechanism of membrane damage mediated by human eosinophil cationic protein. *Nature 321*, 613−616.
21. Tschopp, J., Podack, E. R., and Muller-Eberhard, H. J. (1982) Ultrastructure of the membrane attack complex of complement: detection of the tetramolecular C9-polymerizing complex C5b-8. *Proc. Natl. Acad. Sci. U.S.A. 23*, 7474−7478.
22. Futami, J., Maeda, T., Kitazoe, M., Nukui, E., Tada, H., Seno, M., Kosaka, M., and Yamada, H. (2001) Preparation of potent cytotoxic ribonucleases by cationization: enhanced cellular uptake and decreased interaction with ribonuclease inhibitor by chemical modification of carboxyl groups. *Biochemistry 40*, 7518−7524.
23. Maeda, T., Kitazoe, M., Tada, H., de Llorens, R., Salomón, D. S., Ueda, M., Yamada, H., and Seno, M. (2002) Growth inhibition of mammalian cells by eosinophil cationic protein. *Eur. J. Biochem. 269*, 307−316.
24. Harder, J., and Schröder, J. M. (2002) RNase 7, a novel innate immune defense antimicrobial protein of healthy human skin. *J. Biol. Chem. 277*, 46779−46784.
25. Zhang, J., Dyer, K. D., and Rosenberg, H. F. (2003) Human RNase 7: a new cationic ribonuclease of the RNase A superfamily. *Nucleic Acids Res. 31*, 602−607.
26. Chen, B., and Przybyla, A. (1994) An efficient site-directed mutagenesis method based on PCR. *Biotechniques 17*, 657−659.
27. Barlett, G. R. (1959) Colorimetric assay methods for free and phosphorylated glyceric acids. *J. Biol. Chem. 234*, 466−468.
28. Ellens, H. J., Bentz, J., and Szoka, C. (1985) H^+- and Ca^{2+}-induced fusion and destabilization of liposomes. *Biochemistry 6*, 1948−1954.
29. de los Rios, V., Mancheño, J. M., Lanio, M. E., Oñaderra, M., and Gavilanes, J. G. (1998) Mechanism of the leakage induced on lipid model membranes by the hemolytic protein sticholysin II from the sea anemone *Stichodactyla helianthus*. *Eur. J. Biochem. 252*, 284−289.
30. Abagyan, R., Totrov, M., and Kuznetsov, D. (1994) ICM-A new method for protein modeling and design: application to docking and structure prediction from the distored native conformation. *J. Comp. Chem. 15*, 488−506.

31. Koradi, R., Billeter, M., and Wuthrich, K. (1996*)* MOLMOL: a program for display and analysis of macromolecular structures. *J. Mol. Graph. 14*, 29−32.
32. Mallorquí-Fernández, G., Pous, J., Peracaula, R., Aymamí, J., Maeda, T., Tada, H., Yamada, H., Seno, M., de Llorens, R., Gomis-Rüth, F. X., and Coll, M. (2000) Three- dimensional crystal structure of human eosinophil cationic protein (RNase 3) at 1.75 Å resolution. *J. Mol. Biol. 300*, 1297−1307.
33. Boix, E., Nogués, M. V., Schein, C. H., Benner, S. A., and Cuchillo, C. M. (1994) Reverse transphosphorylation by ribonuclease A needs an intact p2-binding site. Point mutations at Lys-7 and Arg-10 alter catalytic properties of the enzyme. *J. Biol. Chem. 269*, 2529−2534.
34. Braun, P., and von Heijne, G. (1999) The aromatic residues Trp and Phe have different effects on the positioning of a transmembrane helix in the microsomal membrane. *Biochemistry 38*, 9778−9782.
35. Rozek, A., Friedrich, C. L., and Hancock, R. E. W. (2000) Structure of the bovine antimicrobial peptide indolicidin bound to dodecylphosphocholine and sodium dodecyl sulfate micelles. *Biochemistry 39*, 15765−15774.
36. Yau, W. M., Wimley, W. C., Gawrisch, K., and White, S. H. (1998) The preference of tryptophan for membrane interfaces. *Biochemistry 37*, 14713−14718.
37. Abu-Ghazaleh, R. I., Gleich, G. J., and Prendergast, F. G. (1992) Interaction of eosinophil granule major basic protein with synthetic lipid bilayers: a mechanism for toxicity. *J. Membr. Biol. 128*, 153−164.
38. Dathe, M., Meyer, J., Beyermann, M., Maul, B., Hoischen, C., and Bienert, M. (2002) General aspects of peptide selectivity towards lipid bilayers and cell membranes studied by variation of the structural parameters of amphipathic helical model peptides. *Biochim. Biophys. Acta 1558*, 171−186.
39. Ladokhin, A. S., and White, S. H. (2001) Protein chemistry at membrane interfaces: nonadditivity of electrostatic and hydrophobic interactions. *J. Mol. Biol. 309*, 543−552.
40. Friedrich, C. L., Moyles, D., Beveridge, T. J., and Hancock, R. E. W. (2000) Antibacterical action of structurally diverse cationic peptides on gram-positive bacteria. *Antimicrob. Agents Chemother. 44*, 2086−2092.
41. Zhang, L., Rozek, A., and Hancock, R. E. W. (2001) Interaction of cationic antimicrobial peptides with model membranes. *J. Biol. Chem. 276*, 35714−35722.
42. Gudmundsson, G. H., and Agerberth, B. (1999) Neutrophil antibacterial peptides, multifunctional effector molecules in the mammalian immune system. *J. Immunol. Methods 232*, 45−54.
43. Gouet, P., Courcelle, E., Stuart, D. I., and Metoz, F. (1999) *ESPript: in PostScript. Bioinformatics 15*, 305−308.

BI0273011